Landscape Evolution of the Alps: A Review of the State of Knowledge and New Results from Morphometric Analysis

Master Thesis

zur Erlangung des akademischen Grades

Master of Science

der Studienrichtung Geosciences

an der Universität Graz

verfasst von

Gerit Albert Gradwohl

01213183

betreut von

Kurt Stüwe

Graz, Februar 2020

Abstract

The European Alps are one of the most famous mountain ranges on Earth. Being one of the best studied orogens in the world, surprisingly little is known about the exact formation of its landscapes or the age of its topography. This thesis summarizes the state of knowledge on topography, uplift history and landscape formation of the range. Different approaches and techniques are used to showcase and date these aspects. For example, (i) morphometric analysis show disequilibrium features of major drainages and that the Alps are characterized by decreasing slopes at high elevations with no difference between Eastern and Western Alps. (ii) Sediment fluxes to the surrounding basins started about 35 Ma and show a substantial increase since the Pliocene. (iii) Thermochronometric data yield strongly accelerated exhumation since the Pleistocene. (iv) Surface dating via ^{10}Be and ^{26}Al records a young incision history for the last 4 to 5 Myr. Integrating these different datasets into a model for the geological uplift history shows that topographic evolution for the last 45 Ma was happening rather slowly until about 5 Ma and accelerated thereafter. Neither tectonics nor climate can be made responsible to be the sole reason for the young uplift, but rather a combination of both. For example, for the Western Alps some 50 % of the surface uplift may be attributed to climatic driven erosion in the Pliocene. Conversely, in the Eastern Alps, abundant relict landscapes at high elevations indicate a long wavelength tectonic driver at depth.

Zusammenfassung

Die Europäischen Alpen sind einer der bekanntesten Gebirgszüge der Welt. Obwohl die Alpen eines der am besten untersuchten Orogene sind, ist erstaunlich wenig über die genaue Entstehung der dort anzufindenden Landschaften oder das Alter der Topografie bekannt. Diese Arbeit fasst den aktuellen Wissenstand über die Topografie, Hebungsgeschichte und Landschaftsentwicklung der Alpen zusammen. Unterschiedliche Techniken und Herangehensweisen werden präsentiert um diese Aspekte aufzuzeigen und zu datieren. (i) Morphometrische Analysen zeigen, dass große Flüsse im Maßstab der Alpen nicht einheitlich equilibriert sind und, dass die Alpen durch eine Reduzierung der Hangneigung mit steigender Höhe charakterisiert sind, ohne systematische Unterschiede zwischen Ost- und Westalpen. (ii) Der Sedimenttransport in die umliegenden Becken begann um 35 Ma und verzeichnet einen starken Anstieg seit dem Pliozän. (iii) Thermochronometrische Daten zeigen eine starke Beschleunigung der Exhumation seit dem Pleistozän. (iv) Oberflächendatierungen mittels ^{10}Be und ^{26}Al signalisieren eine junge Einschneidungsgeschichte über die letzten 4 bis 5 Millionen Jahre. Durch die Zusammenführung dieser unterschiedlen Datensätze in ein Modell für die geologische Hebungsgeschichte ergibt sich, dass die topografische Entwicklung der Alpen über die letzten 45 Millionen Jahre langsam von statten ging und ab 5 Ma rapide beschleunigte. Weder tektonische noch klimatische Faktoren können alleine für die junge Hebung verantwortlich sein, sondern eine Kombination aus beiden. In den Westalpen werden beispielsweise rund 50 % der Oberflächenhebung der klimatisch ausgelösten Erosion zugeschrieben, wohingegen in den Ostalpen das häufige Vorkommen von Reliktlandschaften in großer Höhe auf einen tektonischen Auslöser in der Tiefe mit großer Wellenlänge schließen lassen.

Contents

The majority of this thesis has been submitted to a book with the working title ‘The Alpine Chain’ which is being edited by C. Rosenberg et al. and is expected to be published in 2020.

1 Introduction

The European Alps are one of the most famous and best studied mountain ranges in the world. With some 1000 km in length from Vienna to Marseille, some 250 km in width from Lake Constance to Lake Garda and rising at Mt. Blanc up to 4809 m above sea level, they are the largest and highest mountain range that is located entirely in Europe. The topography of the Alps has been a major obstacle for politically-motivated movements for millennia (Romans, Turkish invasions, modern refugee crisis) and its nature, origin and evolution has attracted geologists and tourists alike for centuries (e.g. Stüwe and Homberger, 2012). Its present state is home to a rich alpine flora and fauna and it acts as an important water supplier for the adjacent countries (Baumgartner et al., 1983). Mountaineers from all over the world come to test their skill by climbing the steep faces of the highest peaks and thanks to the abundance of areas at high enough elevations to have seasons rich in snow, winter-tourism has become one of the most important sources of income for many Alpine regions. As such, the topography of the range and its evolution over geological time are of high interest.

This topography is extremely variable. Apart from steep and high glaciated peak and razor-sharp ridges, the Alps also carry gentle alpine pastures, plateaus and hilly lowlands. In places, these so contrasting environments can be found right next to each other and the varied geological processes that shaped the landscape are obvious to the untrained eye. However, much of their morphology, its evolution over time and the processes that shaped the mountain range are still subject to modern scientific debates.

Historically, the scientific puzzling about the origin of the Alp's topography has led to the birth of some of the most important modern geological and geomorphological concepts, including that of plate tectonics itself, that evolved in the early 20th century by earth scientists in the Alps (Şengör, 2009). Prior to the advent of plate tectonics, mountain ranges like the Alps were thought to be fixed in geographic position and have formed by vertical motions only – a concept that is still entrenched in the intuitive understanding of mountain building by many non-geologists today. Within this so-called 'fixistic' or 'permanence' theory of the 19th century, all land masses are thought to remain in stable position over geological time and topography is simply thought to be the consequence of uplift. The recognition of similar biota on – for example – both sides of the Atlantic, was thought to be caused by wanderings of life forms across land bridges that rise and fall above and below sea level during different periods in geological time. The Central American land bridge between the Americas was thought to be a

modern-day analogue. Although such fixistic thinking was still popular in the 1920s when Hans Stille postulated the various stages of mountain building in terms of 'geosynclinal' theory (Stille, 1919), it had then already been superseded by the interpretation of the Alps in terms of horizontal motions: the theory of nappe tectonics. Eduard Suess (1883) and Marcel Alexandre Bertrand around the same time were among the first to understand that mountain ranges are formed by horizontal transport that exceeds the vertical motions by several orders of magnitude. This concept was consolidated by Wegener (1912), who formulated the theory of continental drift. Undoubtedly, he did so in part because of his love for the mountains of the Alps.

Today, we understand the Alps as the product of plate motions within the modern concepts of geodynamics. The topography of the range is known to be the result of the combined efforts of tectonic and climatic drivers, their dynamic interaction and their feedback processes. The widespread occurrence of metamorphic rocks that are exhumed from many tens of kilometres depth at the surface of the Alps, testifies of the substantial vertical motions that occur during the process of mountain building and we have learned to discriminate between rock uplift and surface uplift (England and Molnar, 1990). We understand the enormous transport capabilities of the major Alpine rivers that have filled the basins surrounding the Aps with kilometre-thick sequences of sediment and we have modern dating tools and digital elevation models to investigate the topography of the range.

Nevertheless, even some of the first order morphological features like the orientation of drainage divides, the age of topography or the geometry of the major drainages present puzzling problems on their origin and geomorphological evolution: Some rivers run through wide, over-deepened valleys, others cut narrow channels through the rock and in places they seem to alternate, as if they were not sure which kind of river they want to be. Lake floors like those of the north Italian lakes reach hundreds of metres below sea level and cannot have been carved by rivers as we see them today and the power of water has created enormous unexplored underground landscapes of caves in the limestone ranges. These and many other geomorphological problems of the Alps are far from being understood.

In this thesis I present aspects of the topography of the Alps and its development over the geological past: the landscape evolution. In describing the topography, I make use of some modern metrics that have not been derived for the Alps on the scale of the mountain range as a whole and summarise some important concepts of its morphology. When describing the

landscape evolution, I present this for the last 45 Ma and introduce some modern discussions on the drivers that shape it today. I begin by presenting a summary of the present topography.

2 The Alps Today

The European Alps are covered by the political territory of seven countries: Austria, France, Germany, Italy, Liechtenstein, Slovenia and Switzerland (Tab. 1). Geographically, the range forms a principal European divide for drainage, climate and culture (Fig. 1a) and, hypsometrically, half of their area are above an elevation of 1500 m above sea level (Fig. 1b). The Alps may be geographically divided into Western, Central, Eastern and Southern Alps. The line separating the Western Alps from the Central Alps runs from the Rhône valley across the St. Bernhard pass into the Aosta valley. The line between Central and Eastern Alps is drawn from Lake Constance in the north to Lake Como in the south, following the Posterior Rhine valley. The line between Eastern and Southern Alps follows the east-west striking valley of Gail, Puster and Adda. Often, this subdivision is simplified by only referring to Western and Eastern Alps, where the term Western Alps is used for the sensu stricto definitions of both Western plus Central Alps. The Swiss Jura, the Bohemian massif and the Slovenian Karst are typically not considered to be part of the Alps, but the Steiner Alps and the Pohorje massif are. Nevertheless, in the south, the Alpine chain merges continuously into the Italian Appenine and in the east into the Dinarides. Except for the boundary between Southern and Eastern Alps, the boundaries described above do not correspond exactly to the geological boundaries between, for example, the Austroalpine and the Penninic domains.

Highest peaks of Alpine countries (order of elevation)	Largest lakes in the Alps	Most important Rivers (catchment over place)
Mont Blanc (4809 m), France	Lake Geneva (581 km^2)	Danube (101300 km^2, Vienna)
Monte Bianco (4809 m), Italy	Lake Constance (541 km^2)	Rhône (100500 km^2, estuary)
Monte Rosa (4634 m), Switzerland	Lago di Garda (370 km^2)	Po (80000 km^2, estuary)
Großglockner (3798 m, Austria	Neusiedler (315 km^2)	Rhine (36200 km^2, Basel)
Zugspitze (2962 m), Germany	Lac de Neuchâtel (218 km^2)	
Triglav (2864 m), Slovenia	Lago Maggiore (212 km^2)	
Vorderer Grauspitz (2599 m), Liechtenstein	Lago di Como (146 km^2)	
	Vierwaldstättersee (114 km^2)	

Tab. 1: Essential geographical facts of the European Alps, showing the highest peak of each Alpine country, the largest Alpine lakes and the most important rivers that drain the Alps.

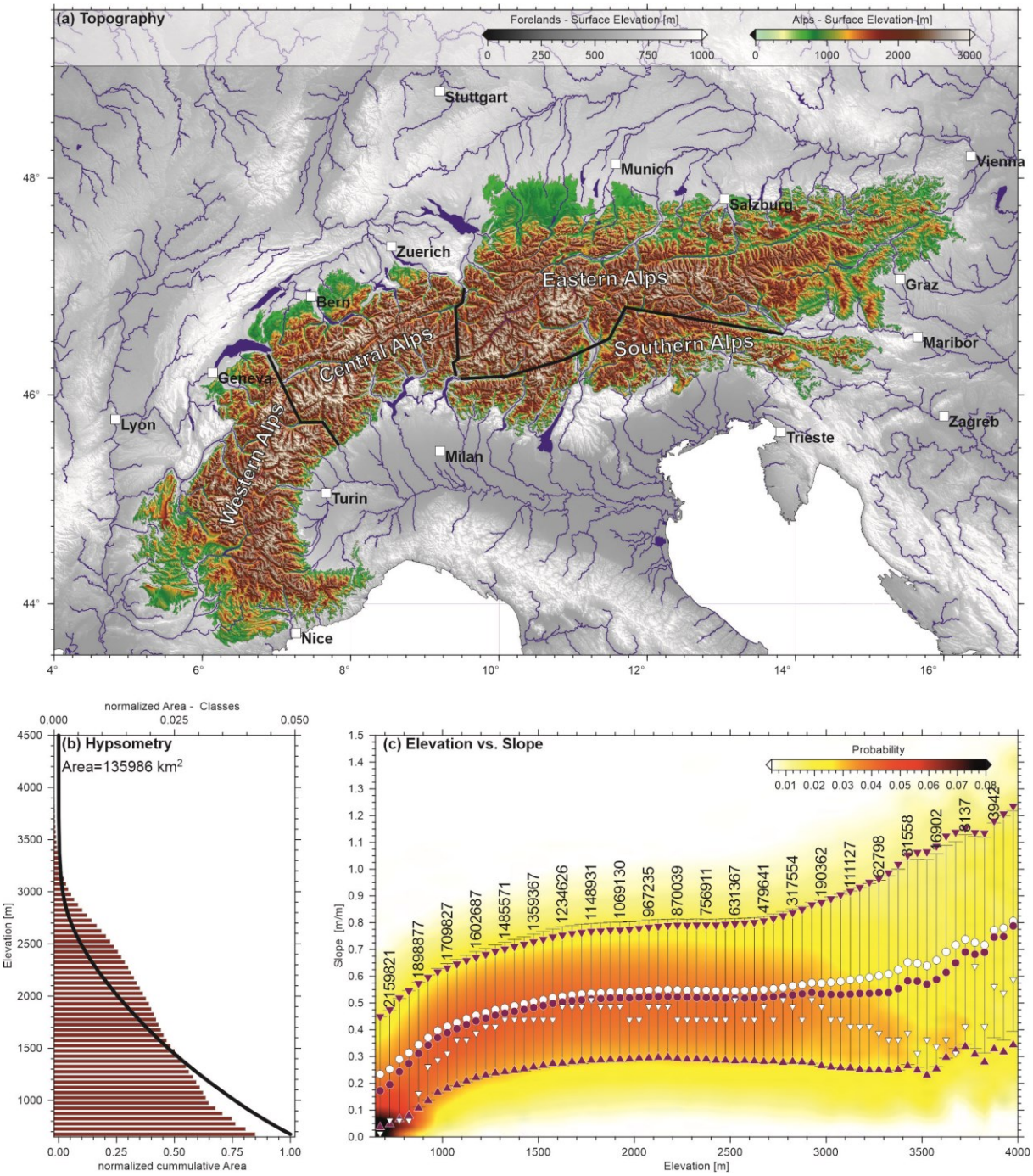

Fig. 1: Topographic metrics of the Alps. (a) Topographic map of the Alps above 650 m above sea level with major rivers and lakes. The borders of Western, Central, Eastern and Southern Alps are indicated with black solid lines. (b) Hypsometric curve of the Alps (solid black line) and normalized area of each elevation class (red bars). (c) Slope – elevation plot of the Alps. White circles with black error bars represent the mean slope and one standard deviation for each 50 m elevation slice. Red circles with red triangles represent the median values (50 percentile) with the 15.8 and 84.1 percentiles. White triangles represent the mode values for each elevation slice. The numbers above every third elevation slice are given.

Morphologically, the Alps are well-known for famous sub-ranges like the Vercors (Mont Aiguille), Bernese Oberland (including the Eiger), the Wallis (including the Matterhorn and Monte Rosa), the High Tauern (Großglockner) and the Lower Tauern and many others. These ranges feature a total of almost 3000 peaks that have a prominence of more than 250 m with

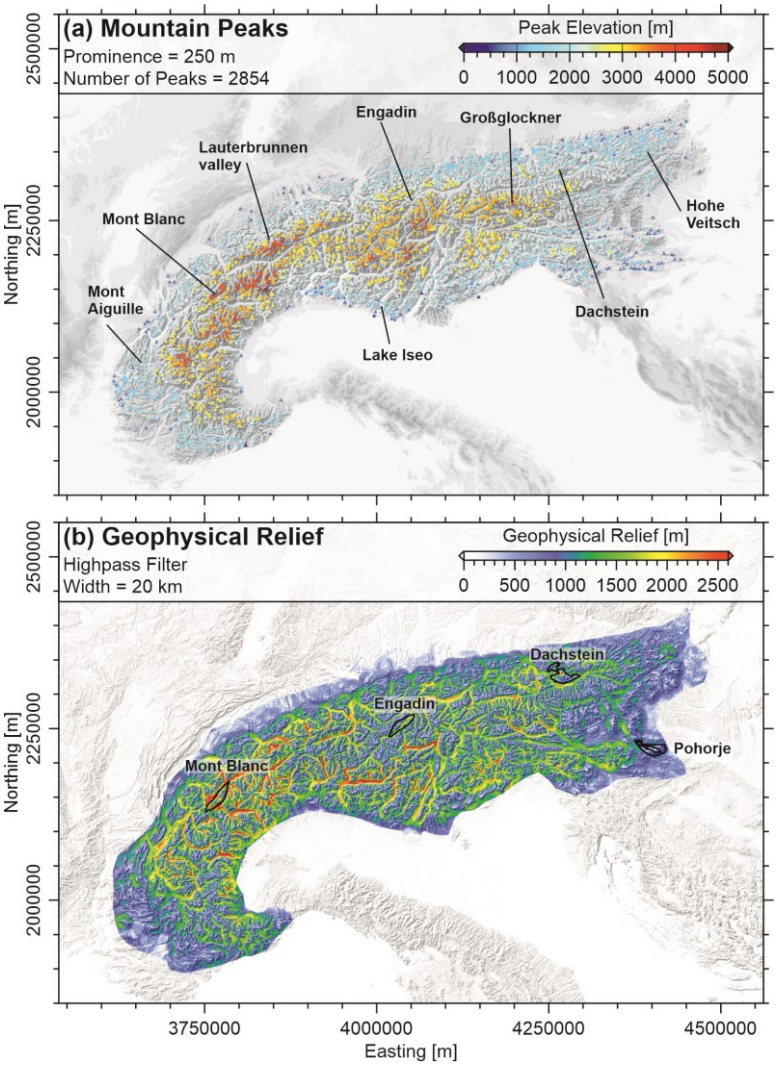

Fig 2: Two maps showing the relief of the Alps. Note, that the highest peaks, as well as the highest relief are located in the Western Alps. (a) Mountain peaks with prominence of at least 250 m. The locations of Fig. 1 are indicated. (b) Geophysical relief from a sliding window with 20 km width. The marked areas correspond to the regions discussed in chapter 3.1.2.

almost 30 of these being above 4000 m in elevation and another 520 of these being at least 3000 m high (Fig. 2a), with most high peaks being located in the Western Alps. Correspondingly, the geophysical relief of the range for a 20 km sized sliding window is up to about 2500 m and is significantly larger in the west than in the east (Fig. 2b).

What defines an alpine landscape are the landforms we encounter when looking at the Alps. Fig. 3 illustrates the enormous variability of landscapes found in the range. Typically, mountains exceeding 3000 m are characterized by a glacial landscape. Ice-filled cirques bordered by steep ridges and horns, as seen, for example, on the Mont Blanc (Fig. 3a). Even though the glaciers are retreating, their distinct morphologies stay visible after the ice has disappeared (Fig. 3b, c). Also, at lower elevations the major drainages of the Alps run in U-shaped valleys that testify of the tracks of enormous masses of ice that shaped these valleys during the glaciation periods (Fig. 3c). Deep Alpine lakes with hundreds of metres of depth formed by the filling of glacial carved valleys with water (Fig. 3d). In contrast, areas that escaped major glacial impact often evidence a more dissected landscape with gullies, ridges and V-shaped valleys (Fig. 3e). One peculiar type of landform of the Alps are the planation surfaces that occur up to 3000 m. These very gentle landscapes are usually bordered by far steeper flanks towards the lowlands and are found in many parts of the Alps, but particularly in the east (Fig. 3f, g, h).

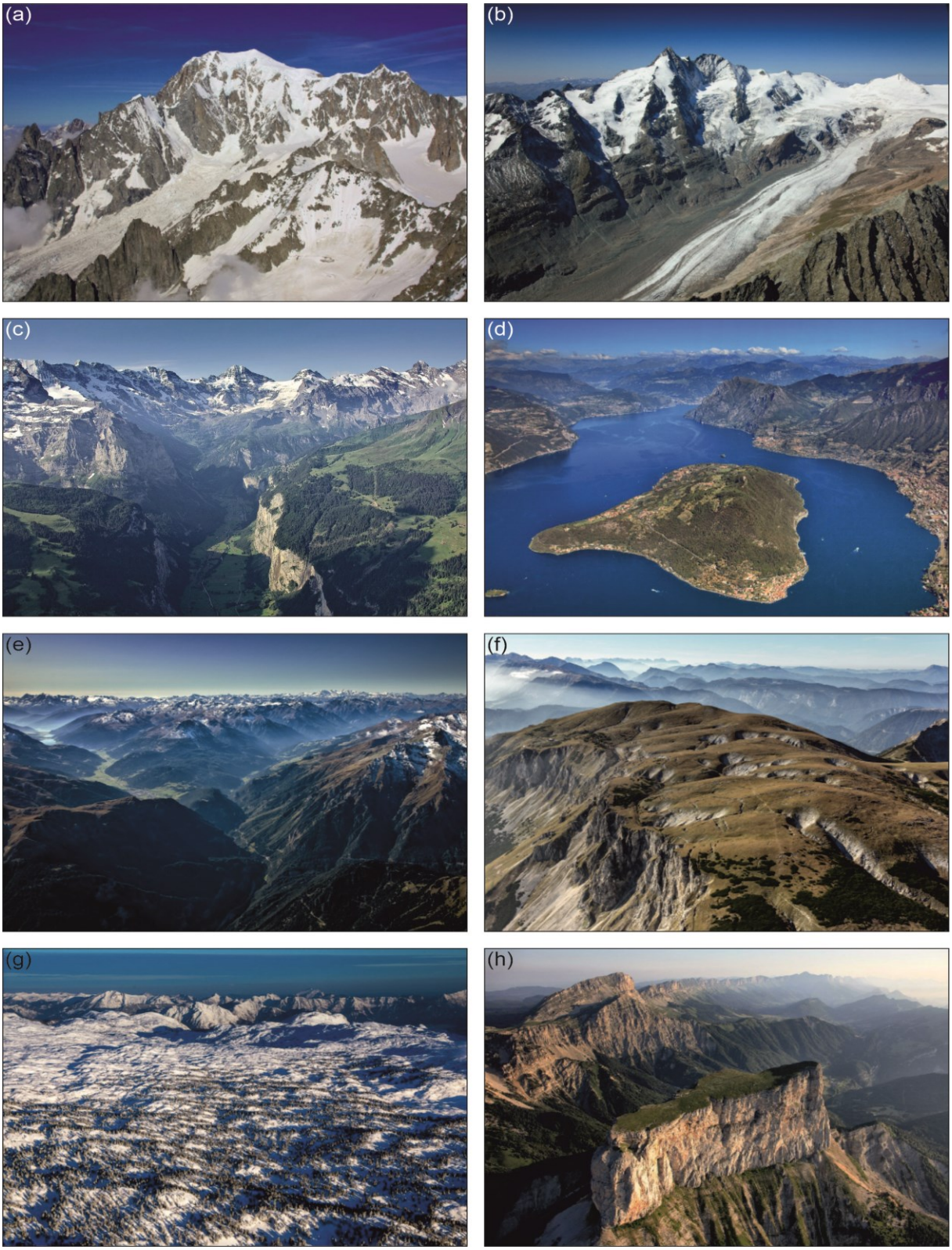

Fig. 3: Photographs from different landscapes across the Alps taken from www.alpengeologie.org (Stüwe and Homberger, 2012) and www.luftbildsteiermark.at (Stüwe and Homberger, 2018). (a) Mont Blanc, the highest peak of the Alps. (b) Großglockner, the highest peak of Austria with the retreating Pasterze glacier. (c) Lauterbrunnen valley, a textbook example of a glacially carved U-shaped valley. (d) Lake Iseo with Montisola island, one of the biggest lake islands of Europe. (e) Engadin region, formerly glaciated mountains that are now characterized by V-shaped valleys, gullies and ridges. (f) Hohe Veitsch in the Hochschwab area, a low relief landscape at high elevation. (g) Dachstein plateau in winter, an example of planation surfaces found in the NCA. (h) Mont Aiguille in the Vercors area, a spectacular high plateau in the Western Alps.

3 Deriving the History of Topography

Landscape is the result of many processes happening at the same time or subsequently to each another. In general, it reflects the current relief as a result of two opposing processes: the production of mass in the form of rock uplift and the removal of mass by extension and/or erosion. When both processes are equal the topography is said to be at geomorphic equilibrium. In the European Alps few landforms bear geomorphic equilibrium features. As such, rock uplift and erosion are not in balance and the history of elevation and topography is not a trivial task to decipher. The main driving force for the initial build-up of topography is the continent-continent collision of the European and the Adriatic lithospheric plate (e.g. Handy et al., 2014). Apart from crustal thickening, isostatic rebound from slab break off processes at depth and rebound from the glaciations in the Pleistocene are the principal processes contributing to rock uplift (Fox et al., 2015). The widespread occurrence of metamorphic rocks at the surface of the Alps shows that these processes are responsible for tens of kilometres of rock uplift. When talking about destruction of topography, glacial and fluvial erosion are the key factors. Both have their typical morphological features and depending on the existing climate one may prevail over the other. How fast the water and/or ice can carve through the rock also depends on the lithology it tries to cut through (e.g. Robl et al., 2015; Stutenbecker et al., 2016). Whatever the details of the denudation processes are, we know that erosion and extension have caused tens of kilometres of denudation from the Alps (England, 1981), so that rock uplift and denudation both have caused comparable amounts of vertical changes in the Alps.

The net elevation of landforms and topography itself is the product of the fine interplay of these processes and is termed uplift (or surface uplift) (England and Molnar, 1990; Stüwe and Barr, 2000). In total, surface uplift is typically only some few percent of the total rock uplift and erosion and is also subject to feedback processes between the two. Indeed, enhanced erosion itself might have had (and still has) its fair share when it comes to uplift in certain areas across the Alps (Champagnac et al., 2009). To figure out which processes led to our present-day relief, we have to take a look at the different data that is available. These include morphometric analysis (section 3.1), sediment budget (section 3.2), thermochronometric data (section 3.3.) and surface dating methods (section 3.4.), but also include direct dating of elevation via paleoaltimetric methods (e.g. Mulch, 2016). However, the latter does not as yet provide well-constrained data and will not be discussed in detail.

3.1 Morphometric Analysis

Analysis of the morphology of the surface topography is clearly one of the most direct and obvious tools to infer its history (e.g. Wobus et al., 2006). Among many other metrics, two specific morphological features have proved to be useful for this: Channel profiles and the statistics of slope-elevation data.

3.1.1 Channel profiles

Rivers and streams do not only showcase the distinct drainage patterns that often go hand in hand with major fault systems (e.g. Keil and Neubauer, 2011) but their longitudinal profiles can also tell us about the dynamics of active deformation (Kirby and Whipple, 2012). Fig. 4 shows channel profiles for the main drainages of the Alps. Rhône and Po flow into the Mediterranean Sea, while Rhine and Danube have the North Sea and the Black Sea as base level, respectively. The Po shows three distinct knickpoints in its channel profile. The fist one occurs ~ 35 km after the source and marks the transition from the Dora-Maira Massif to the Po Plain with a sudden decrease in channel slope. The second knickpoint is located around Torino and shows steeper slopes downstream, which correlates well with post-Miocene activity of thrust faults (Perrone et al., 2013). The last one visible at an orogen-wide scale lies in the area of Piacenza. Slopes are increasing downstream as well. This area is known for recent transpressive tectonic activities, which might explain the knickpoint (Boccaletti et al., 2011). The channel profile of the Rhône until Lyon is strongly influenced by the Pleistocene glacial cycles, which does not allow interpretations in terms of uplift (Cyr et al., 2014) even though the area recently experienced differential uplift (Schlatter et al., 2005). Most deviations from an equilibrium profile fall together with changes in erodibility (Stutenbecker et al., 2016) or glacial geomorphology. Interestingly, the lower portion of the channel profile of the Rhône undercuts the profile of the Rhine. This may be attributed to the major base level drop during the Messinian (Gargani, 2004). Note that the significant drop 40 km downstream of Geneva is caused by human interference with the natural river flow, i.e. the 100 m high Génissiat dam. The Rhine, even though it shares a glacial history as well, shows an equilibrium channel profile from its source to Lake Constance at this scale. Downstream of Lake Constance, it uses the Rhine Graben as a new base level (Uehlinger et al., 2009). The Danube, officially starting in Donaueschingen, does not have its source in the Alpine Chain. Nevertheless, it drains the entirety of the Eastern Alps. When looking at its channel profile, the Danube appears to be somewhat equilibrated until a few kilometres upstream of Passau. There, slopes slightly

increase with the transition from the Molasse Basin to the erosion-resistant rocks of the Bohemian Massif. However, the Danube is an antecedent river which surprisingly cuts through the Bohemian Massif when it could easily stay in the Molasse Basin, which suggests a young uplift history of the region.

A more detailed description of the method and the different channel profiles can be found in the Appendix.

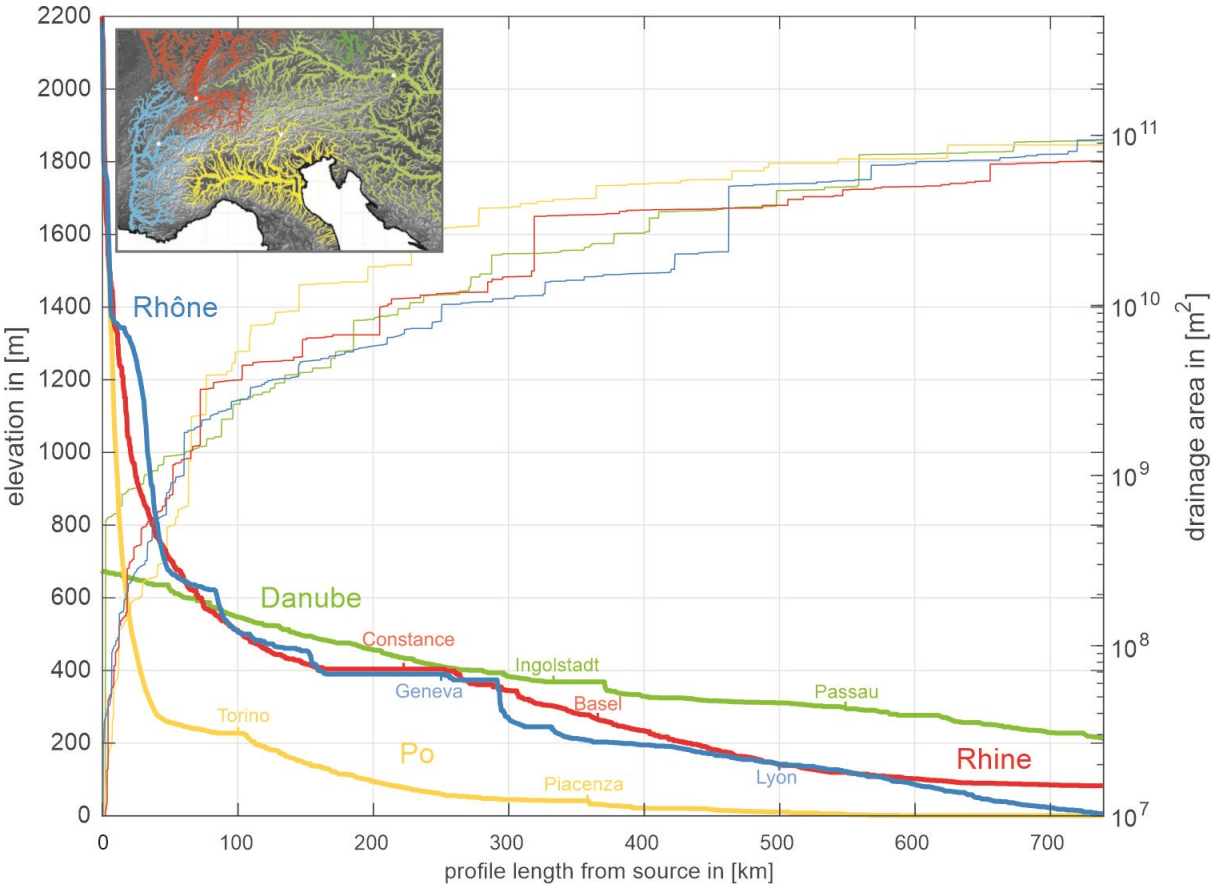

Fig. 4: Channel profiles of the four largest drainages of the Alps: Po (yellow), Rhône (blue), Rhine (red) and Danube (green). The inset shows the tributary network of these four rivers in their according colours.

3.1.2 Slope-elevation statistics

A good tool to put numbers on topography is the relationship of slope and elevation. Hergarten et al. (2010) were the first modern study that recognised that the mean slope of the Alps decreases with elevation, by using an approach that normalises slope for catchment size. They suggested three possible interpretations for this unusual relationship that is not found in many other mountain belts: (i) higher erosion rates at high surface elevations, maintaining equilibrium by high erosion on less steep slopes, (ii) absence of uplift at high elevations, maintaining equilibrium by low erosion rates, and (iii) geomorphic disequilibrium due to immature

topography. They suggested that immature topography is the best idea, because the highest parts of the Alps show low erodibility and high threshold slopes and recent uplift rate measurements show no decrease of uplift rates in high areas.

Robl et al. (2015) recognised that this is similar when considering all slopes, even without consideration of catchment size. When performing this analysis for the entire European Alps (Fig. 1c) an increase in slope up to about 1800 m is visible. Above this elevation up to about 2900 m the mean and median slopes remain constant at about 27°. For elevations higher than 2900 m an increase in slope up to 39° at summit regions is possible, but the mode values decrease up until 3700 m. This is comparable to the findings of Kühni and Pfiffner (2001), who found 25° between 1700 m and 2700 m to be the threshold value for the Swiss Alps. A clear difference in trend between Eastern and Western Alps is not apparent. However, when looking at slope-elevation plots of specific areas with varying glacial history and landform persistence (lithology) different trends are visible that may possibly be interpreted in terms of different uplift or erosion histories. In Fig. 4 four selected examples of Alpine topography are depicted in terms of slope and elevation that differ with respect to tectonics, lithology and glacial history.

The Mont Blanc Massif (Fig. 1a, Fig. 5a) represents an alpine landscape with strong glacial imprint and is characterized by trunk valleys, cirques and extremely high topography. At lower elevations a high frequency of both high and low slopes can be seen. This bimodal landscape is typical for trunk valleys with their flat valley floors and steep flanks. The highest mode values for slope are found at elevations between 1500 m and 2000 m which roughly coincides with the proposed equilibrium line altitude (ELA) of the last glacial maximum (LGM) (Ivy-Ochs et al., 2006, 2008). Above this altitude where spacious cirques start to occur, topographic gradients decrease. The slope-elevation distribution is therefore consistent with a landscape formed by glaciers.

The Engadin region (Fig. 1e, Fig. 5b) was glaciated several times during the Pleistocene as well but it does not show the same abundance of glacial landforms as the Mont Blanc anymore. Instead, numerous gullies and channels dissect the surface indicating a fluvial erosional regime. Remaining glacial landforms are only locally observed. The slope-elevation distribution starts with very low topographic gradients at the valley floor and steepens along glacially formed flanks. A maximum in slope is reached at about 1100 m followed by relict planation surfaces on valley shoulders at about 1300 m. Above this altitude slopes increase up to the summit regions. Since the Engadin region lacks a wide range of topographic gradients due to missing

glacial landforms, it shows generally lower slopes compared to the Mont Blanc Massif. Comparing these two areas, the persistence (and therefore the decay rate) of non-equilibrium landforms shows a strong lithology dependence with higher erodible rocks in the Engadin region.

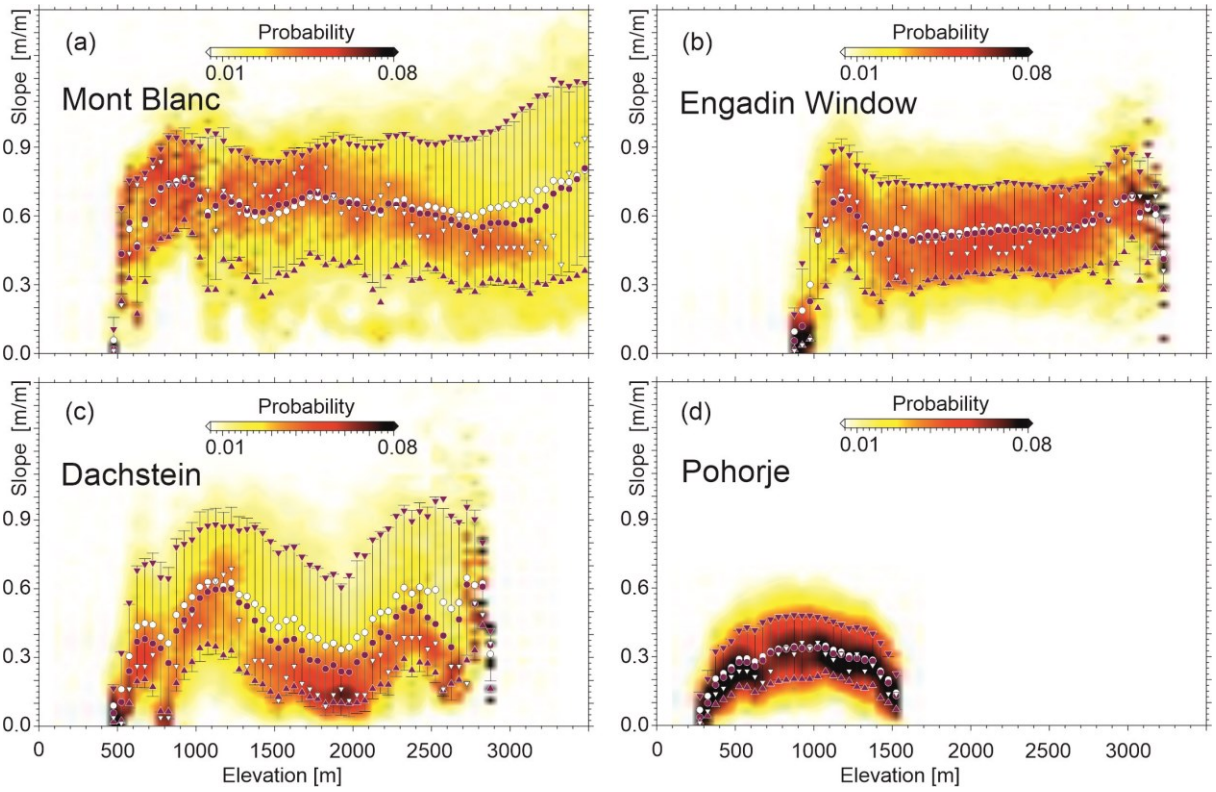

Fig. 5: Slope – elevation plots of four areas across the Alps from Robl et al. (2015). (a) Mont Blanc region. (b) Engadin region. (c) Dachstein. (d) Pohorje. Rough locations for these regions are shown in Fig. 2b. For further information see text.

The Dachstein Massif (Fig. 1g, Fig. 5c) represents an alpine landscape with glaciation history but low surface process rates. Due to the abundance of karstification most run-off happens underground, which leads to low surface erosion rates. The low topographic gradients at 500 m and 700 m represent the valley floors north and south of the Dachstein Massif, respectively. Between 900 m and 1400 m the slopes show bimodal behavior, bearing the highest mean and mode values. Planation surfaces and steep near-vertical walls mark this elevation range. Between 1400 m and 2100 m very low slopes occur which correlates with a fluvial gravel-bearing paleo-surface of inferred Oligocene age (Frisch et al., 2001). In the Northern Calcareous Alps many elevated planation surfaces are known to contain these fluvial gravels. The relief steepens up until 2500 m but slopes decrease again at the glaciated regions near the summit. The reduction of surface run-off through karstification nicely shows the lithology dependence of landform persistence.

The Pohorje Massif (Fig. 5d) is shown here as a region that is representative for a region that was never glaciated during the Pleistocene glaciation cycles. It consists of steep, incised channels at low altitudes with knickpoints separating them from the higher, gentle headwaters where a spacious paleo-surface occurs (Robl et al., 2008a; Legrain et al., 2014a). Between 300 m and 500 m a strong increase in slope occurs followed by a significant drop in mean and mode values between 500 m and 700 m. This low topographic gradient correlates with the occurrence of a dry and wide Drava river parallel valley. Then slopes increase again until 1000 m. In this elevation range deeply incised valleys occur. Above 1000 m slopes decrease significantly towards the peaks where paleo-surfaces dominate. Note the low standard deviation when compared to the decreasing slope values with elevation of the Mont Blanc Massif.

3.2 Sediment Budget

As soon as topography rises, erosion will try to compensate this state of disequilibrium through increased erosion rates until a new state of equilibrium is established (Champagnac et al., 2012). Higher erosion results in increased sedimentation into the adjacent basins. Thus, sediment budgets from surrounding sedimentary basins may be interpreted in terms of the history of topography. The Alps are surrounded by five major sedimentation basins that accommodate the sediments that have been eroded off the range since the onset of surface topography formation in the Oligocene. These basins include the Northern and Southern Molasse Basins, the Pannonian Basin, the Rhône Delta in the Tyrrhenian Sea and the Danube Delta in the Black Sea. England (1981) already recognized that the sediment volumes of these basins can be used to constrain the exhumation process and aspects of topography development.

When looking at the sediment budget of Alpine catchments in more detail, past erosion rates can be determined with high temporal but low spatial resolution (Kuhlemann et al., 2002). Changes in erosion rates can have multiple controlling factors. Apart from the relief in the geologic past, changes in base level (eustatic sea-level change), climate change and differences in erodibility can take important roles for the increase and decrease of sediment discharge. If these factors show minor significance, the sediment budget will be strongly controlled by the relief of the orogen (Einsele, 1992). To find a fitting interpretation for the observed sediment budget of a certain time frame, a comparison with tectonic events, climate and sea level is needed (Kuhlemann, 2007; Willett, 2010).

Fig. 6 shows the sediment yield from the European Alps since the Oligocene split into Eastern and Western Alps (Kuhlemann et al., 2001; Willett, 2010). Since the oldest sediments in the Molasse basin show late Eocene ages, this age appears to be a good starting point to evaluate the sedimentary fluxes of the Alps. The first significant change occurred around 30 – 28 Ma with a doubling of sediment accumulation rates. This was correlated with collision and slab break-off of the Penninic oceanic lithosphere below the Periadriatic line at depth (von Blanckenburg and Davies, 1995) with resulting surface uplift (Kuhlemann, 2007). Between 24 Ma and 21 Ma the sediment load increased again. This trend is clearly visible for the Western Alps but only slightly visible in the Eastern Alps and is interpreted to correspond to the exhumation of the Aar massif (Schlunegger et al., 1997). The sediment budget of the entire Alps decreased strongly during the Miocene, interrupted by a short increase between 18 Ma and 17 Ma. This is interpreted to be the result of extension with a short phase of decreased lateral extrusion leading to surface uplift. (Frisch et al., 2000). Between 12 Ma and 10 Ma the Eastern Alps show a rise in sediment discharge rates by 35 % not represented in the Western Alps and is at least partly explained by the deceleration of extension (Kuhlemann et al., 2001). At around 5.5 Ma a sharp rise in sediment yield is visible for the Western Alps. This signal seems to be somewhat delayed for the Eastern Alps, showing a less pronounced increase at 4 Ma and a sudden rise in sediment load at around 2 Ma. The reasons for this increase will be discussed in Section 5. The

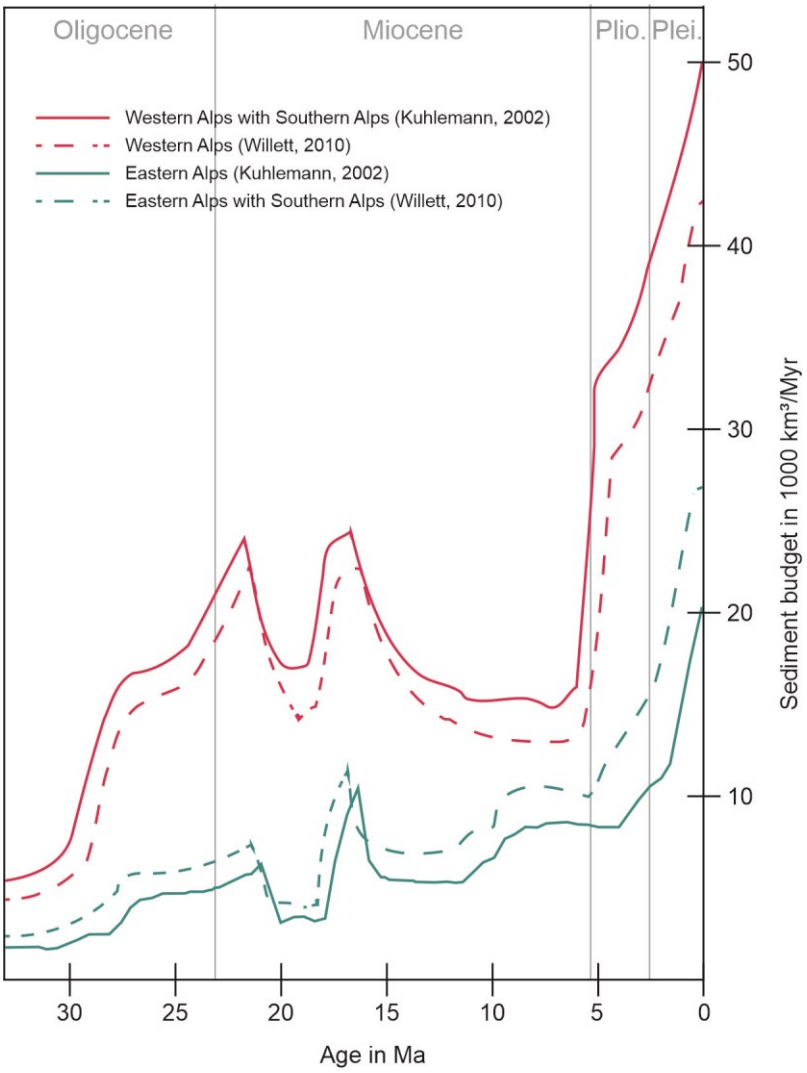

Fig. 6: Sediment budget of the Eastern (blue) and Western (red) Alps over the last 33 Ma from Kuhlemann et al. (2002). The solid lines include the whole of the Southern Alps into the Western Alps (Kuhlemann et al., 2002), while the dashed lines count the sediments derived from the eastern Southern Alps to the Eastern Alps (Willett, 2010).

Western Alps show generally higher cumulative sediment discharge rates than the Eastern Alps but depict similar trends nonetheless. Willett (2010) split the sediment budget of the Southern Alps originally summarized by Kuhlemann et al. (2002) into a western and eastern part and added the latter to the Eastern Alps (Fig. 6). By doing so, the strong increase in sediment yield at ~5.5 Ma becomes also apparent in the Eastern Alps. For the last 5 million years an increase in sediment load at mid to high latitudes is also visible across the globe (Molnar, 2004).

The data and their interpretation presented above are subject to some debate. For example, hiatuses in sedimentation are problematic, since they become harder to identify the further back in time we look. Also, younger sediments did not undergo the same compaction as older sediments. Therefore, sedimentation rates in more recent times seem higher if mentioned factors are ignored (Sadler, 1999). This problem led to voices which argue that the latest Cenozoic sediment record is being overestimated (Schumer and Jerolmack, 2009; Willenbring and von Blanckenburg, 2010).

3.3 Thermochronometric Data

Thermochronometry is the most commonly used tool to constrain the age of landscape and uplift. However, most thermochronometric systems date temperatures along the cooling path and are therefore subject to a series of assumptions on the relationship between cooling and surface uplift, so that the evolution of topography can be inferred. Due to diverse locking temperatures, individual cooling steps can be dated. The main systems used, that are known as low-temperature thermochronometric systems, are: (U-Th)/He in apatite that closes at ~60° C (Farley, 2000), apatite fission tracks at ~110° C (Ketcham et al., 1999), (U-Th)/He in zircon at ~180° C (Reiners et al., 2004) and zircon fission tracks that records ~230° C (Brandon et al., 1998). To obtain the depths of the closure temperatures in the Earth's crust, assumptions of the thermal structure in the past have to be made (Malusà and Fitzgerald, 2019) and the minerals residence time in the partial annealing zone has to be considered (Green et al., 1989). The temporal differences between the dated closure depths give exhumation rates over time (provided that multiple thermochronometric systems are analysed, e.g. Vernon et al., 2008). Erosion rates and incision rates on a Ma timescale can also be determined (e.g. Valla et al., 2011; Legrain et al., 2014a). Furthermore, by looking at cooling histories of not only one spot but also the surrounding areas, exhumation mechanisms can be weighted (e.g. Hejl, 1997).

Many studies have contributed to the pool of low-temperature thermochronometric ages from the Alps (Fig. 7a). A modelled overview of the exhumation rates over the last 32 million years derived from this data set of cooling ages was presented by Fox et al. (2016) (Fig. 7b). This study shows that the first areas to show fast exhumation rates of up to 0.8 km/Myr at 30 Ma lie in the internal arc of the Western Alps. However, it should be noted that significantly older near surface exhumation is known from isolated 'cold spots' in the Eastern Alps (Hejl, 1997).These initial fast exhumation rates decrease significantly to 0.3 km/Myr at around 20 Ma. Simultaneously, exhumation rates across the External Massifs of the Western Alps show an increase to 0.6 km/Myr. The Lepontine Dome and the Tauern Window yield a similar advent of high exhumation rates at 20 Ma. In the Tauern Window, differences between east and west are visible. The eastern and the western Tauern Window show unroofing times of 18 Ma and 15 Ma, respectively. The Glarus region starts to display enhanced exhumation rates at 4 Ma. Looking at the latest evolution, a significant increase in exhumation rates since 2 Myr can be seen in the Western Alps, which is not visible in the Eastern Alps (Fig. 7b). This concerns in particular rapid exhumation in the Mont Blanc and Belledone external Massifs. Model results are somewhat dependent on assumptions of the geothermal gradient and the time step intervals, but the general trend of the exhumation history of the Alps remains the same. Unfortunately, large areas of the Alps do not inherit suitable lithologies for thermochronometric analysis (e.g. Northern Calcareous Alps).

Apart from studying in-situ rocks there is also the possibility to examine thermochronometric ages of sedimentary rocks and sediments of the pro- and retro-side basins of the Alpine wedge. The age difference of the cooling age of the analysed thermochronometric system and the deposition age gives the lag time (Garver et al., 1999; Spiegel et al., 2000). It represents the time that the measured grain needs to travel from the closure depth to the final point of deposition. If the transport time is insignificant compared to the error of the applied method, the lag time reflects erosion rate (Bernet et al., 2004).

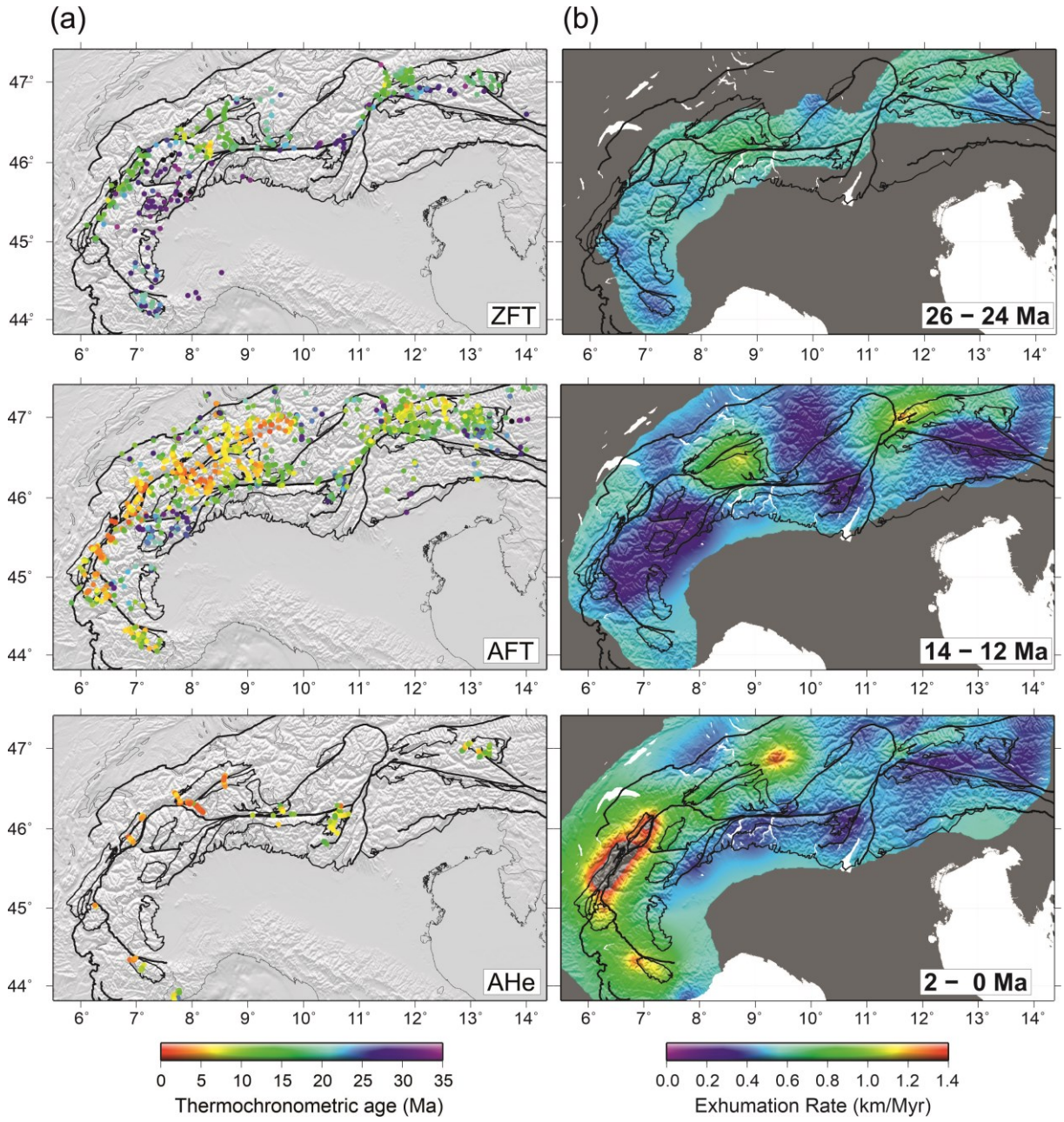

Fig. 7: Low-temperature thermochronometric data across the Alps. (a) Zircon fission track (ZFT), apatite fission track (AFT) and (U-Th)/He in apatite (AHe) data points with their respective ages. (b) Exhumation rates for the time steps 26 – 24 Ma, 14 – 12 Ma and 2 – 0 Ma from a linear inversion model. Adapted from Fox et al. (2016).

3.4 Direct Surface Dating

Direct dating of the surface and its elevation history can be done with paleoaltimetric, OSL, paleontological, sedimentological and a series of other methods. However, one of the most commonly used methods to date landforms near the surface has become the use of cosmogenic isotope methods. Cosmogenically generated isotopes with geological application include the radioactive nuclides ^{10}Be, ^{14}C, ^{26}Al and ^{36}Cl, as well as the stable nuclides ^{3}He and ^{21}Ne (Dunai, 2010; Ivy-Ochs and Kober, 2013). The most used in-situ formed nuclides in the Alps are ^{10}Be

and ^{26}Al in quartz, that have half-lives of 0.7 Ma and 1.5 Ma, respectively. Their production rates as well as the ratio of their production rates in quartz are well known and show a simple depth dependence with an e-folding penetration depth of some 60 cm (Lal and Arnold, 1985; Nishiizumi et al., 1989; Kubik et al., 1998; Gosse and Phillips, 2001). Apart from telling us the age of the observed surface, in-situ cosmogenic nuclide dating can also help us to reconstruct the rate of its destruction.

Three general ideas are being exploited when making use of these two isotopes: (i) The concentration of ^{10}Be and ^{26}Al may be interpreted in terms of an exposure age. This interpretation assumes instantaneous exposure through the last metres of the rock column. In the Alps aspects like snow cover, vegetation, soil and anthropogenic alteration are difficult to quantify on a 10^4 year time scale and therefore rarely allow this interpretation. (ii) The concentration of ^{10}Be and ^{26}Al may be interpreted in terms of continuous accumulation during erosion-driven exhumation of the last few metres, that is, in terms of erosion rate (von Blanckenburg, 2005). (iii) Finally, the time that has passed since the measured grain was last exposed to cosmic rays, representing the decay of cosmogenic nuclides, may be interpreted as burial age (Granger and Muzikar, 2001). The error on these ages is usually in the range of 5 %. However, the fast decay rates of these cosmogenic radionuclides limit these dating methods to approximately 5 Ma.

Erosion rate measurements on a 10^4 time scale using ^{10}Be have been performed for a series of regions in the Alps (e.g. Wittmann et al., 2007; 2016; Norton et al., 2008; 2010; Glotzbach et al., 2013). They vary widely between 0.05 mm/yr and 2 mm/yr with a distinct trend of higher erosion ratees in glaciated regions and lower rates (typically below 0.1 mm/yr) in regions that escaped Pleistocene glaciation (Dixon et al., 2016;). There are many factors controlling erosion rates such as lithology, precipitation, temperature, mean basin slope or changes in base level. In general, erosion rates depend on the erodibility of the rock and climate. However, these factors mostly represent local erosional environments and their weighting might differ completely when comparing different areas. Thus, correlation of orogen-scale erosion rates remains challenging.

Burial age dating efforts in the Alps are very limited, but due to the abundance of karst caves at various topographic levels, this method is likely to advance our understanding of uplift history in the future. Many caves record phreatic-vadose transitions and bear siliceous sediments, so that ^{26}Al/^{10}Be ratios can be used to date their formation as a proxy for uplift of the Alps. An

example where cave levels ranging from 558 m a.s.l. up to 1800 m a.s.l. have been dated using ^{10}Be and ^{26}Al, is the Siebenhengste-Hohgant cave system in Switzerland (Häuselmann, 2007; Häuselmann et al., 2007; Fig. 8). For the cave level at 1800 m the oldest burial age they found was 4.4 Ma. By sampling several speleogenetic levels the valley incision history could be reconstructed, showing rather low incision rates of 0.12 km/Myr before 0.8 Ma and an increase to 1.2 km/Myr thereafter. Interestingly, in a cave at an elevation of 1705 m a.s.l. at Mont Granier in France, a similar burial age of 4.3 Ma was determined (Hobléa et al., 2011; Fig. 8). At the eastern end of the Alps, burial dating has been performed in caves of the never glaciated Grazer Bergland in Austria (Wagner et al., 2010; Fig. 8). They sampled several cave levels up to over 500 m above the local base level and found the oldest burial age to be 4 Ma. The reconstructed incision history shows low mean incision rates of 0.125 km/Myr for the last 4 Ma. When looking at the data in more detail, incision rates show a drastic decrease since 2.5 Ma, contrasting the latest valley evolution in the Swiss Alps (Häuselmann, 2007). Interestingly, the incision rates at the eastern fringe of the Alps compare quite well with the incision rates of the Swiss Alps before 0.8 Ma. These incision rates in the Grazer Bergland region may also be directly interpreted in terms of surface uplift rates of the surrounding highlands because it is observed that the principal drainages of the region are antecedent streams that transect the

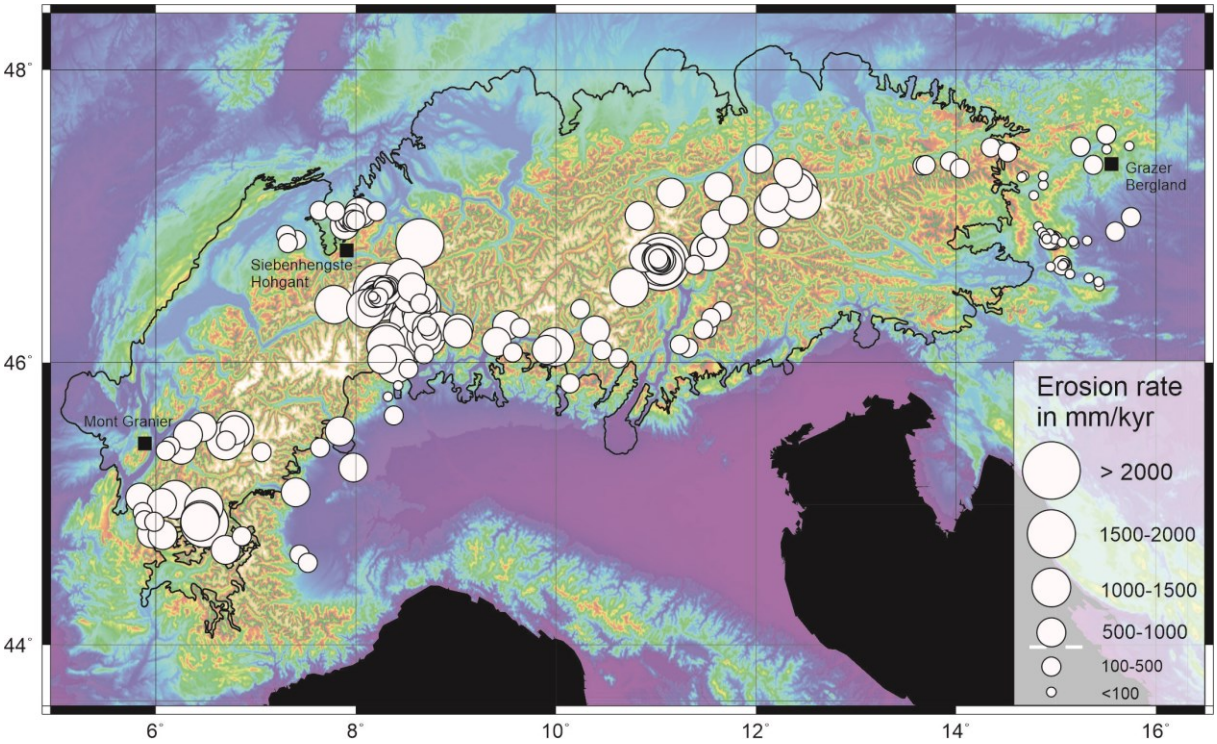

Fig. 8: Cosmogenic nuclide-derived erosion rates on a 10^4 year time scale across the Alps. Note that the unglaciated eastern end of the Alps shows significantly lower erosion rates than the rest of the range. Produced from the data compilation of Dixon et al. (2016).

Alpine orogen – Pannonian basin base level transition without knickpoint. Wagner et al. (2011) also correlated planation surfaces of the area with sampled cave levels, constraining their age as well. This correlation is only possible when erosion rates have been low enough to allow direct comparison of elevations. By backward modelling the number of nuclides prior to burial, paleo-erosion rates can be gauged (assuming the local production rates of ^{10}Be and ^{26}Al). This approach resulted in low pre-burial erosion rates of ~20 m/Myr for sediments in the sampled caves from Wagner et al. (2011).

4 Landscape Evolution since the Eocene

The methods described in the last section allows to reconstruct aspects of the landscape evolution of the Alps over the last 45 Myr (Fig. 9; see also: Schuster and Stüwe, in print). Quite generally, it may be said that the formation of the present-day landscape and topography started with the termination of subduction of the Penninic ocean. Even though the distribution of land and sea differed strongly from today, remnants of landscapes from this time can still be found in the Alps.

In the middle Eocene (~ 45 Ma, Fig. 9a), the last remains of the northern Penninic ocean (Valais domain) were not yet entirely subducted. In the area of the modern Eastern Alps, however, the Adriatic plate started to thrust onto the southern European margin. This led to uplift of the Austroalpine and the formation of a flexural foreland basin (northern Molasse Basin) and its subsequent flooding by the Paratethys Sea. The topography on the non-marine European plate was characterized by flat lowlands. The uplifted Austroalpine probably formed a hilly topography at this time that started eroding and peneplanation over the next 10 Myr or so. This led to the formation of the oldest landforms preserved today in the Eastern Alps: the plateaus on the Northern Calcerous Alps, that much later started hosting the Augenstein landscape (see Oligocene time slice below) or the well-known Nockfläche in the Niedere Tauern (Exner, 1949). The fact that low temperature thermochronometric ages reaching back up to 50 Ma are still preserved, suggests low topography and erosion rates for Eocene landscapes in the Alps.

During the late Eocene (~ 37 Ma, Fig. 9b) the closure of the Penninic ocean had been completed and the Alpine orogenic wedge also started to thrust over the Helvetic platform in the modern Western Alps with a few millimetres per year. Most of the areas of the modern Alps had already emerged from the sea. According to thermochronometric data, most of the medium grade metamorphic rocks from the Alpine metamorphic event were still buried several kilometres, with only few areas in the east being exhumed in the early to middle Paleogene (Hejl, 1997).

In the early Oligocene (~ 30 Ma, Fig. 9c) the ongoing loading of the southern European margin by the northward pushing Adriatic plate caused further subsidence of the shelf areas and a northward shift of the shoreline north of the Paratethys Sea (Frisch et al., 1998). Rifting of the Rhine Graben, which is still active today, commenced and caused subsidence in that area. The most important event for the uplift history of the Alps, however, was the break-off of the subducted Penninic slab underneath the western part of the Alps. This caused an uneven uplift

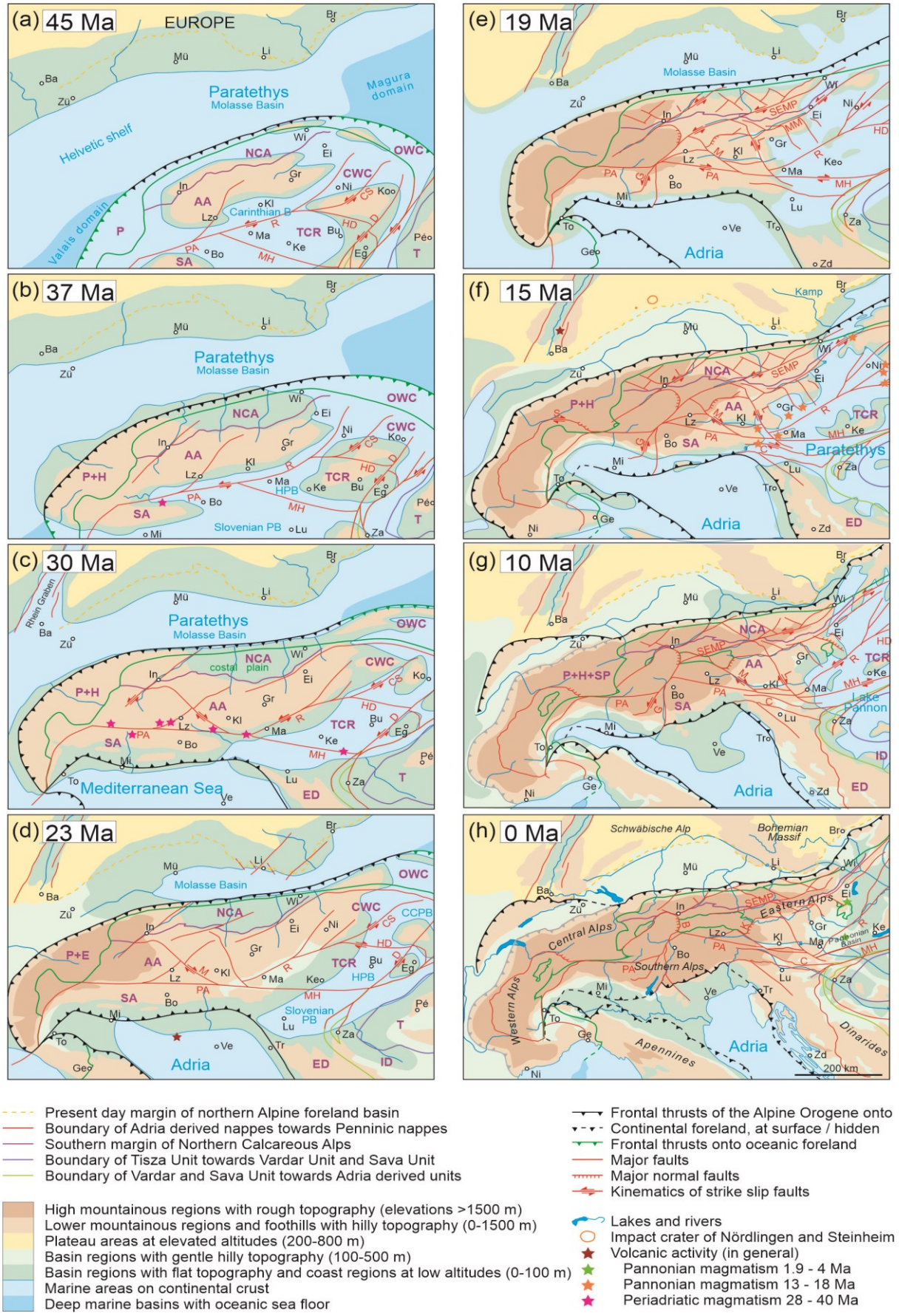

Fig. 9: Tectonic and topographic evolution of the Alps since 45 Ma. After Schuster and Stüwe (in print) but with an extension to the west. For details, see text.

regime across the range: While the Western Alps experienced accelerated uplift, the Eastern Alps east of the Inntal fault, together with the Western Carpathians, formed hilly lowlands terminating in coastal plains bordering the Paratethys Sea (Frisch et al., 1998). On the plateaus of the Northern Calcareous Alps, remnants of these coastal plains are still preserved as conglomerates and (redeposited) gravels, also called the Augenstein Formation (Frisch et al., 2001). The peneplanation of these surfaces on Triassic rocks indicates that these plains followed some relief in earlier times. All major rivers of the Eastern Alps drained to the north into the northern Molasse Basin at this time. The Periadriatic Fault changed its shear sense from sinistral to dextral right after the intrusion of the main Periadriatic plutons and associated volcanism (Mancktelow et al., 2001).

From late Oligocene to early Miocene (~ 23 Ma, Fig. 9d) the removal of the Penninic slab caused further surface uplift of the Western Alps with the development of the first mountainous regions from the Inn valley westwards (Frisch et al., 1998; 2001). This increased topography gave rise to enhanced erosion and thus exhumation (Kuhlemann et al., 2001). Not only the highlands were rising, also the western Molasse Basin underwent significant uplift. This caused the area north of the Western Alps to fall dry. In the east, the last remnant of Penninic oceanic lithosphere subducted westwards underneath the present-day Carpathians.

In the early Miocene (~ 19 Ma, Fig. 9e) the subducting plate underneath the Carpathian Arc began rolling-back rapidly to the east (Royden et al., 1983; Ren et al., 2012). The opened space was filled by the adjacent continental units, including the Alpine orogenic wedge. This led to lateral extrusion of the Alps, causing the formation of the major orogen-parallel strike-slip faults, which govern the present-day drainage pattern of the Eastern Alps (Ratschbacher et al., 1991; Frisch et al., 1998; Robl et al., 2008b; Wölfler et al., 2011; Bartosch et al., 2017). Contemporaneous to crustal thinning in the easternmost part of the Alps and the Pannonian region, north-south shortening of the Adriatic Indenter led to crustal thickening in the Tauern Window region (Ratschbacher et al., 1989). Enhanced erosion due to higher topography and extensional detachments perpendicular to the Alpine orogen initiated accelerated exhumation of the Lepontine Dome (Simplon) and the Tauern Window (Brenner, Katschberg) (Mancktelow, 1992; Fügenschuh et al., 1997; Wölfler et al., 2011; 2012). The continuing loading of the Eurasian plate by the propagating Alpine orogenic wedge led to subsidence north of the Alps. The northern Molasse Basin was subsequently flooded again by the redevelopment of the sea arm connecting the Paratethys and the Mediterranean Sea. The orogen adjacent basins were substantially filled with sediment due to enhanced erosion (Kuhlemann et al., 2001).

During the middle Miocene (~ 15 Ma, Fig. 9f) the thrusting of the orogenic wedge over the Eurasian plate had stopped and was replaced by convergence of the two plates. This led to crustal thickening and hence further uplift of the Alps. The Lepontine dome, the Aar and Gotthard Massifs, as well as the Tauern Window show increased exhumation rates, while the western External Massifs stay at lower rates, indicating foreland propagation at a later time for the westernmost Alps (Fox et al., 2016). In addition to the change in tectonic regime, the climate got colder and caused a global sea level drop due to the accretion of the Antarctic ice shield. This caused the Molasse basin to successively fall dry from east to west. The still ongoing eastward extension led to the formation of several intermontane basins by fault-controlled pull-apart processes along the east-west oriented strike-slip faults defining the drainage network of the Eastern Alps (Bartosch et al., 2017). At the same time these basins were filled by local clastic sediments, the Paratethys transgressed south of the Alps to the west, flooding the easternmost basins and forming a narrow connection to the Adriatic Sea. The fact that some of these intramontane basins bear marine sediments shows that the mean elevation was still not substantial. The effects of lateral extrusion were less severe in the west.

In late Miocene times (~ 10 Ma, Fig. 9g) east-west extension had declined in the east due to termination of the subduction underneath the Carpathian Arc, causing onset of basin inversion and uplift (Bada et al., 2007). The brackish remnants of the isolated western Paratethys, known as Lake Pannon, formed the eastern boarder of the modern Alps. The central and eastern Northern Calcareous Alps became substantially uplifted and started to erode (Frisch et al., 1998). In the Western Alps, the Mont Blanc, Aiguille Rouge and Belledonne External Massifs were still buried at kilometres depth but now show accelerated exhumation (Fox et al., 2016).

In the latest Miocene, most important event that affected the topography of the Alps occurred in the Messinian (~6 Ma). The Mediterranean Sea got isolated from the open ocean due to tectonic closure of the waterways to the Atlantic Ocean and ice accumulation in the Arctic causing the water table to drop (e.g. Krijgsman et al., 1999). This led to the desiccation of the Mediterranean Sea and the formation of evaporites from highly saline waters. The Messinian Salinity Crisis was responsible for the biggest area of dry land below sea-level known so far. The drop in base level also significantly increased incision of rivers draining into the Mediterranean Sea, creating the deep valleys which confine the lakes at the southern border of the Alps (Bini et al., 1978; Finckh, 1978) and abnormal channel profiles for large rivers like the Adige (Robl et al., 2008a). The influence of a lowered base level can also be seen in the Rhône

valley (Gargani, 2004). The event terminated with the flooding of the Mediterranean Sea around 5.3 Ma.

From the Pliocene until today (5.3 Ma – 0 Ma, Fig. 9h), the Alps now underwent serious build-up of topography. Erosion rates show a significant increase since 5 Ma (Kuhlemann, 2007). At the eastern border of the Alps surface uplift of at least 500 m can be seen (Wagner et al., 2010; Legrain et al., 2014b, b). Around the same time, relateable incicion rates from the western and northwestern border are known (Häuselmann, 2007; Häuselmann et al., 2007; Hobléa et al., 2011). Hergarten et al. (2010) inferred that 40 % of the time and uplift needed to reach geomorphological equilibrium were attained. With the onset of major glaciation in the Alps during the Pleistocene, the carving of U-shaped valleys and cirques with steep faces dominated the processes sculpting the landscape. In combination with surface uplift also visible in the non-glaciated parts of the Alps, these young glacial cycles are responsible for most of our alpine landforms today. But the Alps are far from being done growing. Vertical displacements measured with GPS/GNSS stations show growth rates exceeding 2 mm/yr (Sternai et al., 2019; Fig. 10). However, it is noted that interpolations of GPS-determined uplift rates as shown in Fig. 10 are, in part, inconsistent with geological evidence for uplift, for example at the eastern end of the Alps.

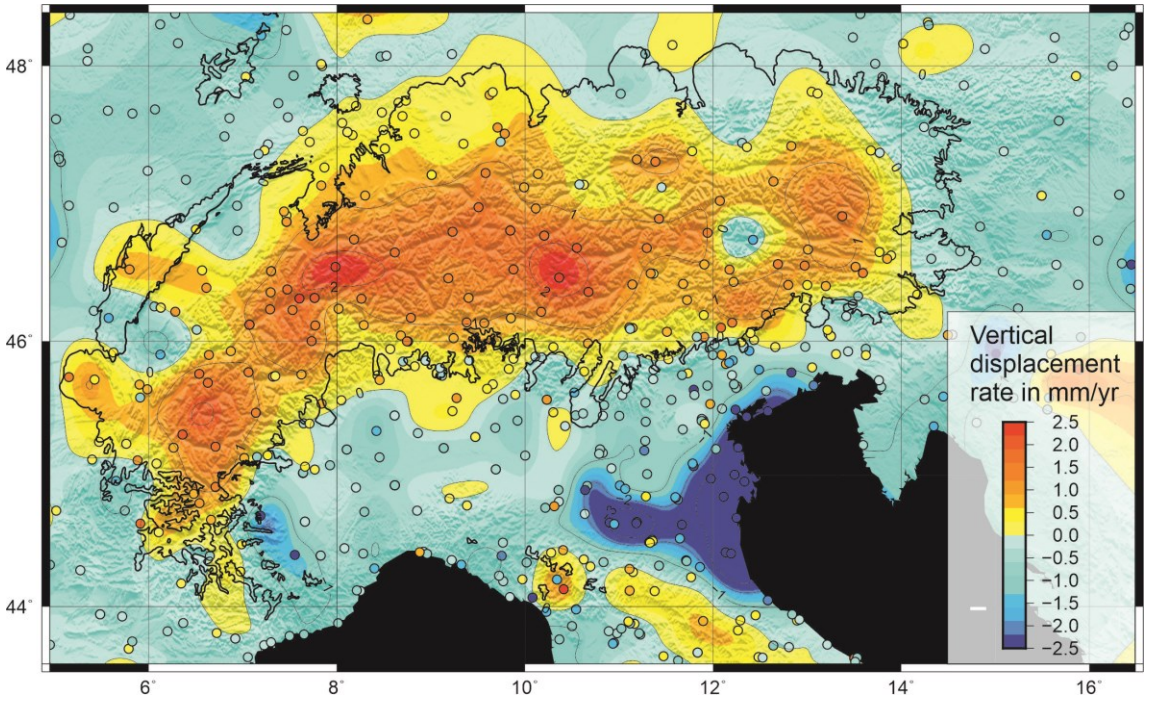

Fig. 10: Present-day vertical displacement rates measured with GPS/GNSS across the Alps, modified from the interpretation of Sternai et al. (2019). Circles indicate the location of the measuring GPS/GNSS stations.

5 Drivers of Topography and Landscape Evolution

In view of the surface uplift history described in the last sections, the question about the underlying drivers arises quickly. Clearly, the evolution of a landscape mirrors the counterplay between uplift and erosion. Even in one of the best studied mountain ranges in the world, assessing the drivers of the evolution of our observed topography is still fuelling active debates on this topic (e.g. Baran et al., 2014; Dixon et al., 2016; Sternai et al., 2019). The two opposing stands argue about whether the young uplift and increase in denudation rates is mainly due to climatic or tectonic control. These two drivers have been discussed for time slices as old as the Oligocene (Schlunegger and Norton, 2015), but I focus here on the last substantial uplift pulse at post-Miocene times.

The tectonic control may best be understood by summarising todays deformation regime. The current rotation pole of the Adriatric microplate with respect to the European plate is generally placed within the Western Alps and the western Po Basin (e.g. Calais et al., 2002; Weber et al., 2010) with a counter-clockwise rotational motion, although some studies like Le Breton et al. (2017) found a counter-clockwise rotation of Adria relative to Europe of 5° about a finite Euler Pole in southern Spain to be the best fit. The rotational motion results in different deformation regimes across the Alps: transtension or minor compression in the Western Alps, dextral shear in the Central Alps and compression in the Eastern Alps (e.g. Sue et al., 2007; Walpersdorf et al., 2015; Serpelloni et al., 2016). This compression is evidenced by rapid uplift at the eastern end of the Alps (Robl et al., 2008a; Wagner et al., 2010, 2011; Legrain et al., 2014b) which is, coincidentally, inconsistent with the interpretation of Sternai et al., (2019; Fig 11). The relative motion is likely to have been similar since at least the early Pliocene when it is known that deformation in the Central Alps due to north-south convergence stopped (Schmid et al., 1996) and the locus of uplift and exhumation migrated into the core of the orogen (Fox et al., 2016; Fig. 7). At depth, teleseismic tomography implies a southward dipping lithospheric slab underneath the Central Alps, a detached European slab underneath the Western Alps and a reversal in subduction polarity underneath the Eastern Alps with a northeastward-dipping Adriatic slab (Lippitsch et al., 2003), or even potential slab detachment underneath the Eastern Alps as well (Qorbani et al., 2015).

The climatic control is governed by a continuous cooling of the atmosphere since the mid Miocene thermal maximum (Zachos et al., 2001). At the end of the Miocene this cooling accelerated during the Messinian and ultimately resulted in glaciation of the Alps in the

Pleistocene. The Miocene-Pliocene transition was also characterized by a change to wetter conditions and the desiccation of the Mediterranean from 5.8 – 5.3 Ma and a dramatic increase in erosional fluxes into the sedimentary basins surrounding the Alps (Willett et al., 2006; Fig. 6). Increased erosional fluxes around this time are in fact observed globally (Molnar, 2004).

The global increase of sediment fluxes at 5 Ma (Molnar, 2004) would lead to the conclusion, that a change in climate was the main driver for uplift, since no global tectonic phenomena are known for that time. For the Alps, this is in fact the conclusion of Willett et al. (2006) and Champagnac et al. (2007) who argue that the climate change with wetter climate since the Messinian accounts for some 50% of the surface uplift. Such an interpretation implies that this surface uplift is predominantly seen in the peaks, with most erosion occurring in the valleys and the mean elevation of the range actually decreasing. Champagnac et al. (2007) used the geophysical relief of the Western Alps (see also Fig. 2b) to argue that this is the case. Champagnac et al. (2008) showed how this erosion driven rebound is also responsible for the tilting of some foreland regions. Such tilting and erosion of the foreland basin was also recognised by Cederbom et al. (2004) who extrapolated this tilting into the orogen to argue that some 6.5 km were eroded there since the Pliocene. Nevertheless, in general it is agreed that not 100% of the uplift and exhumation in the central axis of the Alpine orogen can be attributed to these climatic drivers. As deformation is known to have ceased at the time of these processes, deep seated drivers in the lithosphere are likely to be partly responsible for these vertical motions in the central orogen, showing that both, tectonic and climatic drivers contribute to uplift.

In the Eastern Alps, deep seated tectonic drivers as the principal cause of a long wavelength post-Miocene uplift event have been argued for some time (e.g. Lippitsch et al., 2003; Genser et al., 2007; Wagner et al., 2010; Robl et al., 2015). There, relict landscapes with channel knickpoints which still need to migrate towards the headwaters can be found (Fig. 11). Correlations with different cave levels record a young uplift of some 500 m since > 4 Ma (Robl et al., 2008a; Wagner et al., 2010, 2011; Legrain et al., 2014b). These regions show no signs of areal glaciation, which allows the interpretation of juvenile landscapes due to recent uplift. However, too little surfaces across the Alps were dated this way to enable assumptions covering the whole range. Interestingly, elevated high relief surfaces in the Eastern Alps can be found in areas that were glaciated as well as unglaciated during the LGM, for example the Augenstein

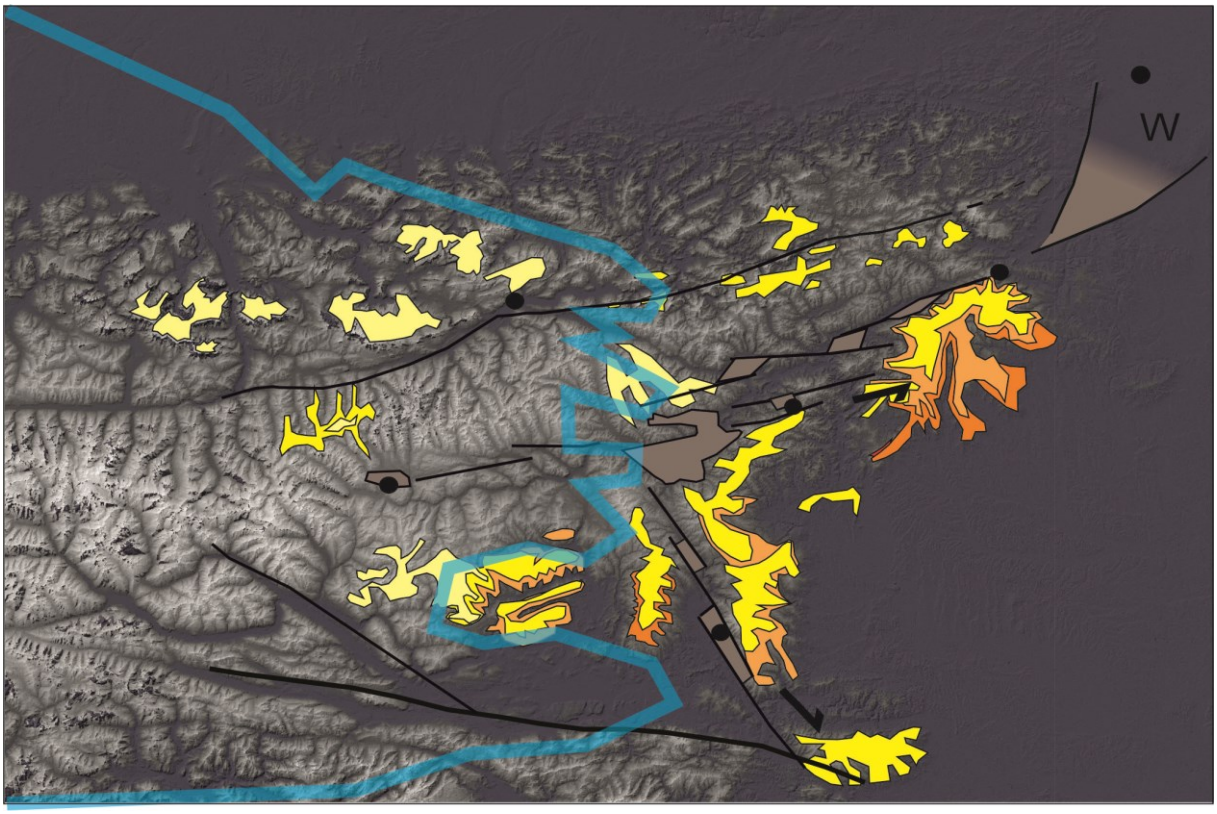

Fig. 11: Simplified schematic map of the planation surfaces in the Eastern Alps (from Winkler-Hermaden, 1957; Hejl, 1997; Frisch et al., 2001; Wagner et al., 2011; Legrain et al., 2014a; Bartosch and Stüwe, 2019). Wagner et al. (2011) provided some correlation of some of these surfaces. According to them, the shown surfaces correspond roughly to the Dachstein surface (light yellow) at about 2500 m a.s.l., the Nock, or Kor-surface (bright yellow), the Woscheneck or Hubenhalt levels (light orange), and the lower levels that are known as the Trahütten, Hochstraden, Stadelberg/Zaraberg levels below about 600 m above base level.

landscape of the NCA or the Nockfläche in the Niedere Tauern region. To entangle the influence of glaciers and a possible young uplift pulse on these landscapes, further efforts regarding the coverage of mapped and dated planation surfaces, combined with numerical landscape evolution modelling have to be made in the future.

A similar discussion goes on about an even younger time: the shaping of today's morphology during and after the glaciation periods. While it is clear that the glaciations caused some major re-organisation of the drainage system in some places (Robl et al., 2008a), it is also observed that major U-shaped valley use much earlier defined valley courses (Montgomery and Korup, 2011). Nevertheless, there is an ongoing discussion on the drivers of low relief landscapes, in particular due to the unusual slope-elevation relationship discussed above (Fig. 1, 5). In particular, it is being discussed if these are caused by glacial processes or are relics of old uplifted surfaces.

When looking at recent erosion rates, the differences between Western and Eastern Alps is not abundant, except for the unglaciated easternmost part, where erosion rates are significantly

lower (Dixon et al., 2016; Fig. 4). These erosion rates are dependent on the erosional regime, which is primarily governed by climate. Glacial erosion is more effective than fluvial erosion and is often used to explain an increase in erosion rates, e.g. by lowering the ELA (e.g. Häuselmann et al., 2007). Apart from lowering the ELA by generally decreasing the mean annual temperature, increased glaciation can also be achieved by uplifting lower areas above the existing ELA. In this case tectonics have a direct impact on the local climate and could initiate the beforementioned feedback loop of erosion and uplift. When encountering combinations of fluvial and glacial erosion, e.g. a U-shaped valley with a V-shape at the bottom, the fluvial incision is usually dated after the glaciation event. However, since implausible high erosion rates would be needed to explain the incision after glaciation, some gorges are believed to have formed contemporary or even before glacial advance (Montgomery and Korup, 2011).

6 Conclusions

In this thesis I presented a number of state-of-the-art research methods and their applications to derive the age and evolution of landscapes and surface elevation of the scenic mountain range of the European Alps. Combining all the gathered information, I come to the following conclusions.

- The landscape evolution of the Alps started about 35 Ma, but some landforms can be traced back to about 45 Ma. However, the surface uplift in the Alps was not happening linearly since the Oligocene. Recent studies show that a substantial part of the uplift is as young as the Pliocene. Deep lithospheric processes appear to be the best explanation for this in the Eastern Alps, but in the Western Alps a substantial portion of this has been attributed to climatic drivers.
- Even if recent sediment fluxes are being overestimated due to sampling effects, a sudden rise in sediment fluxes to the sedimentary basins surrounding the Alps since the Pliocene seems out of question. It correlates well with the young uplift and incision observed in both, the Eastern and Western Alps.
- The existence of planation surfaces, particularly in the Eastern Alps, is interpreted to be the reflection of an immature geomorphological state and the young uplift since the Pliocene. The occurrence of these surfaces in regions with differing glacial history remains puzzling and deserves further investigation.
- Since the onset of Pleistocene glaciations, the Alps got reshaped with an abundance of glacial features. Major reorganization of drainages, which still govern a big part of the mountain range, occurred.
- Despite the difference in geophysical relief, the slope-elevation distribution and erosion rates do not show a clear trend differentiating the Eastern Alps from the Western Alps. A bimodal distribution of low slopes at low and high elevations is unusual in comparison with many other mountain belts. Minor differences may depend on the varying glacial histories.

Acknowledgements

I thank M. Fox, R. Schuster and P. Sternai for kindly sharing their working files from their publications to produce Figs. 7, 9 and 11, respectively. I also thank T. Bartosch for helping me to create the channel profiles and R. Watson for handing over a well sorted pool of literature on the topic. Most importantly, I thank my supervisor Kurt Stüwe who has motivated me to develop an understanding for the dynamics of the Earth like nobody else has. Thank you for all the help and advices I received over the time and all the good times in the field, it is highly appreciated. This work was financially supported by the Austrian Science Fund (FWF-project P31609-NBL).

References

Bada, G., Horváth, F., Dövényi, P., Szafián, P., Windhoffer, G., Cloetingh, S., 2007. Present-day stress field and tectonic inversion in the Pannonian basin. Glob. Planet. Change 58, 165–180. https://doi.org/10.1016/j.gloplacha.2007.01.007

Baran, R., Friedrich, A.M., Schlunegger, F., 2014. The late Miocene to Holocene erosion pattern of the Alpine foreland basin reflects Eurasian slab unloading beneath the western Alps rather than global climate change. Lithosphere 6, 124–131. https://doi.org/10.1130/L307.1

Bartosch, T., Stüwe, K., 2019. Evidence for pre-pleistocene landforms in the eastern alps: Geomorphological constraints from the gurktal alps. Austrian J. Earth Sci. 112, 84–102. https://doi.org/10.17738/ajes.2019.0006

Bartosch, T., Stüwe, K., Robl, J., 2017. Topographic evolution of the Eastern Alps: The influence of strike-slip faulting activity. Lithosphere 9, 384–398. https://doi.org/10.1130/L594.1

Baumgartner, A., Reichelt, E., Weber, G., 1983. Der Wasserhaushalt der Alpen. Niederschlag, Verdunstung, Abfluß und Gletscherspende im Gesamtgebiet der Alpen im Jahresdurchschnitt für die Normalperiode 1931-1969. Oldenbourg, München, Wien.

Bernet, M., Brandon, M.T., Garver, J.I., Molitor, B., 2004. Downstream Changes of Alpine Zircon Fission-Track Ages in the Rhone and Rhine Rivers. J. Sediment. Res. 74, 82–94. https://doi.org/10.1306/041003740082

Bini, A., Cita, M.B., Gaetani, M., 1978. Southern Alpine lakes - Hypothesis of an erosional origin related to the Messinian entrenchment. Mar. Geol. 27, 271–288. https://doi.org/10.1016/0025-3227(78)90035-X

Boccaletti, M., Corti, G., Martelli, L., 2011. Recent and active tectonics of the external zone of the Northern Apennines (Italy). Int. J. Earth Sci. 100, 1331–1348. https://doi.org/10.1007/s00531-010-0545-y

Brandon, M.T., Roden-Tice, M.K., Carver, J.I., 1998. Late Cenozoic exhumation of the Cascadia accretionary wedge in the Olympic Mountains, northwest Washington State. Bull. Geol. Soc. Am. 110, 985–1009. https://doi.org/10.1130/0016-

7606(1998)110<0985:LCEOTC>2.3.CO;2

Calais, E., Nocquet, J.M., Jouanne, F., Tardy, M., 2002. Current strain regime in the Western Alps from continuous Global Positioning System measurements, 1996-2001. Geology 30, 651–654. https://doi.org/10.1130/0091-7613(2002)030<0651:CSRITW>2.0.CO;2

Cederbom, C.E., Sinclair, H.D., Schlunegger, F., Rahn, M.K., 2004. Climate-induced rebound and exhumation of the European Alps. Geology 32, 709–712. https://doi.org/10.1130/G20491.1

Champagnac, J.D., Molnar, P., Anderson, R.S., Sue, C., Delacou, B., 2007. Quaternary erosion-induced isostatic rebound in the western Alps. Geology 35, 195–198. https://doi.org/10.1130/G23053A.1

Champagnac, J.D., Molnar, P., Sue, C., Herman, F., 2012. Tectonics, climate, and mountain topography. J. Geophys. Res. Solid Earth 117. https://doi.org/10.1029/2011JB008348

Champagnac, J.D., Schlunegger, F., Norton, K., von Blanckenburg, F., Abbühl, L.M., Schwab, M., 2009. Erosion-driven uplift of the modern Central Alps. Tectonophysics 474, 236–249. https://doi.org/10.1016/j.tecto.2009.02.024

Champagnac, J.D., Van Der Beek, P., Diraison, G., Dauphin, S., 2008. Flexural isostatic response of the Alps to increased Quaternary erosion recorded by foreland basin remnants, SE France. Terra Nov. 20, 213–220. https://doi.org/10.1111/j.1365-3121.2008.00809.x

Cyr, A.J., Granger, D.E., Olivetti, V., Molin, P., 2014. Distinguishing between tectonic and lithologic controls on bedrock channel longitudinal profiles using cosmogenic 10Be erosion rates and channel steepness index. Geomorphology 209, 27–38. https://doi.org/10.1016/j.geomorph.2013.12.010

Dixon, J.L., von Blanckenburg, F., Stüwe, K., Christl, M., 2016. Glaciation's topographic control on Holocene erosion at the eastern edge of the Alps. Earth Surf. Dyn. 4, 895–909. https://doi.org/10.5194/esurf-4-895-2016

Dunai, T.J., 2010. Cosmogenic Nuclides. Cambridge University Press, Cambridge, (198 pp.). https://doi.org/10.1017/CBO9780511804519

Einsele, G., 1992. Sedimentary Basins: Evolution, Facies and Sediment Budget, Springer-

Verlag, Berlin, Heidelberg (628 pp.). https://doi.org/10.1093/gji/119.3.1018

England, P., 1981. Metamorphic pressure estimates and sediment volumes for the Alpine orogeny: an independent control on geobarometers? Earth Planet. Sci. Lett. 56, 387–397. https://doi.org/10.1016/0012-821X(81)90142-4

England, P., Molnar, P., 1990. Surface uplift, uplift of rocks, and exhumation of rocks. Geology 18, 1173–1177. https://doi.org/10.1130/0091-7613(1990)018<1173:SUUORA>2.3.CO;2

Exner, C., 1949. Beitrag zur Kenntnis der jungen Hebung der östlichen Hohen Tauern. Mitt. Geogr. Ges. Wien 91, 186–196.

Farley, K.A., 2000. Helium diffusion from apatite: General behavior as illustrated by Durango fluorapatite. J. Geophys. Res. Solid Earth 105, 2903–2914. https://doi.org/10.1029/1999jb900348

Finckh, P.G., 1978. Are southern Alpine lakes former Messinian canyons? - Geophysical evidence for preglacial erosion in the southern Alpine lakes. Mar. Geol. 27, 289–302. https://doi.org/10.1016/0025-3227(78)90036-1

Fox, M., Herman, F., Kissling, E., Willett, S.D., 2015. Rapid exhumation in the Western Alps driven by slab detachment and glacial erosion. Geology 43, 379–382. https://doi.org/10.1130/G36411.1

Fox, M., Herman, F., Willett, S.D., Schmid, S.M., 2016. The exhumation history of the European alps inferred from linear inversion of thermochronometric data. Am. J. Sci. 316, 505–541. https://doi.org/10.2475/06.2016.01

Frisch, W., Dunkl, I., Kuhlemann, J., 2000. Post-collisional orogen-parallel large-scale extension in the Eastern Alps. Tectonophysics 327, 239–265. https://doi.org/10.1016/S0040-1951(00)00204-3

Frisch, W., Kuhlemann, J., Dunkl, I., Brügel, A., 1998. Palinspastic reconstruction and topographic evolution of the Eastern Alps during late Tertiary tectonic extrusion. Tectonophysics 297, 1–15. https://doi.org/10.1016/S0040-1951(98)00160-7

Frisch, W., Kuhlemann, J., Dunkl, I., Székely, B., 2001. The Dachstein paleosurface and the Augenstein Formation in the Northern Calcareous Alps - A mosaic stone in the

geomorphological evolution of the Eastern Alps. Int. J. Earth Sci. 90, 500–518. https://doi.org/10.1007/s005310000189

Fügenschuh, B., Seward, D., Mancktelow, N., 1997. Exhumation in a convergent orogen: the western Tauern Window. Terra Nov. 9, 213–217. https://doi.org/10.1111/j.1365-3121.1997.tb00015.x

Gargani, J., 2004. Modelling of the erosion in the Rhone valley during the Messinian crisis (France). Quat. Int. 121, 13–22. https://doi.org/10.1016/j.quaint.2004.01.020

Garver, J.I., Brandon, M.T., Roden-Tice, M., Kamp, P.J.J., 1999. Exhumation history of orogenic highlands determined by detrital fission-track thermochronology. Geol. Soc. London, Spec. Publ. 154, 283–304. https://doi.org/10.1144/GSL.SP.1999.154.01.13

Genser, J., Cloetingh, S.A.P.L., Neubauer, F., 2007. Late orogenic rebound and oblique Alpine convergence: New constraints from subsidence analysis of the Austrian Molasse basin. Glob. Planet. Change 58, 214–223. https://doi.org/10.1016/j.gloplacha.2007.03.010

Glotzbach, C., Van Der Beek, P., Carcaillet, J., Delunel, R., 2013. Deciphering the driving forces of erosion rates on millennial to million-year timescales in glacially impacted landscapes: An example from the Western Alps. J. Geophys. Res. Earth Surf. 118, 1491–1515. https://doi.org/10.1002/jgrf.20107

Gosse, J.C., Phillips, F.M., 2001. Terrestrial in situ cosmogenic nuclides: theory and application. Quat. Sci. Rev. 20, 1475–1560. https://doi.org/10.1016/S0277-3791(00)00171-2

Granger, D.E., Muzikar, P.F., 2001. Dating sediment burial with in situ-produced cosmogenic nuclides: theory, techniques, and limitations. Earth Planet. Sci. Lett. 188, 269–281. https://doi.org/10.1016/S0012-821X(01)00309-0

Green, P.F., Duddy, I.R., Laslett, G.M., Hegarty, K.A., Gleadow, A.J.W., Lovering, J.F., 1989. Thermal annealing of fission tracks in apatite 4. Quantitative modelling techniques and extension to geological timescales. Chem. Geol. Isot. Geosci. Sect. 79, 155–182. https://doi.org/10.1016/0168-9622(89)90018-3

Handy, M.R., Ustaszewski, K., Kissling, E., 2014. Reconstructing the Alps–Carpathians–Dinarides as a key to understanding switches in subduction polarity, slab gaps and surface

motion. Int. J. Earth Sci. 104, 1–26. https://doi.org/10.1007/s00531-014-1060-3

Häuselmann, P., 2007. How to date nothing with cosmogenic nuclides. Acta Carsologica 36, 93–100. https://doi.org/10.3986/ac.v36i1.212

Häuselmann, P., Granger, D.E., Jeannin, P.Y., Lauritzen, S.E., 2007. Abrupt glacial valley incision at 0.8 Ma dated from cave deposits in Switzerland. Geology 35, 143–146. https://doi.org/10.1130/G23094A

Hejl, E., 1997. "Cold spots" during the Cenozoic evolution of the Eastern Alps: Thermochronological interpretation of apatite fission-track data. Tectonophysics 272, 159–173. https://doi.org/10.1016/S0040-1951(96)00256-9

Hergarten, S., Wagner, T., Stüwe, K., 2010. Age and Prematurity of the Alps Derived from Topography. Earth Planet. Sci. Lett. 297, 453–460. https://doi.org/10.1016/j.epsl.2010.06.048

Hobléa, F., Häuselmann, P., Kubik, P., 2011. Cosmogenic nuclide dating of cave deposits of Mount Granier (Hauts de Chartreuse Nature Reserve, France): morphogenic and palaeogeographical implications. Géomorphologie Reli. Process. Environ. 17, 395–406. https://doi.org/10.4000/geomorphologie.9607

Ivy-Ochs, S., Kerschner, H., Reuther, A., Maisch, M., Sailer, R., Schaefer, J., Kubik, P.W., Synal, H.-A., Schlüchter, C., 2006. The timing of glacier advances in the northern European Alps based on surface exposure dating with cosmogenic ^{10}Be, ^{26}Al, ^{36}Cl, and ^{21}Ne, in: Siame, L.L., Bourlès, D.L., Brown, E.T. (Eds), In Situ-Produced Cosmogenic Nuclides and Quantification of Geological Processes. Geol. Soc. Am. Special Paper 415, p. 43–60. https://doi.org/10.1130/2006.2415(04)

Ivy-Ochs, S., Kerschner, H., Reuther, A., Preusser, F., Heine, K., Maisch, M., Kubik, P.W., Schlüchter, C., 2008. Chronology of the last glacial cycle in the European Alps. J. Quat. Sci. 23, 559–573. https://doi.org/10.1002/jqs.1202

Ivy-Ochs, S., Kober, F., 2013. Exposure Geochronology, in: Elias, S.A., Mock, C.J. (Eds), Encyclopedia of Quaternary Science: Second Edition. Elsevier, Amsterdam, p. 432-439. https://doi.org/10.1016/B978-0-444-53643-3.00034-0

Keil, M., Neubauer, F., 2011. Neotectonics, drainage pattern and geomorphology of the orogen-

parallel Upper Enns Valley (Eastern Alps). Geol. Carpathica 62, 279–295. https://doi.org/10.2478/v10096-011-0022-y

Ketcham, R.A., Donelick, R.A., Carlson, W.D., 1999. Variability of apatite fission-track annealing kinetics; III, Extrapolation to geological time scales. Am. Mineral. 84, 1235–1255. https://doi.org/10.2138/am-1999-0903

Kirby, E., Whipple, K.X., 2012. Expression of active tectonics in erosional landscapes. J. Struct. Geol. 44, 54–75. https://doi.org/10.1016/j.jsg.2012.07.009

Krijgsman, W., Hilgen, F.J., Raffi, I., Sierro, F.J., Wilson, D.S., 1999. Chronology, causes and progression of the Messinian salinity crisis. Nature 400, 652–655. https://doi.org/10.1038/23231

Kubik, P.W., Ivy-Ochs, S., Masarik, J., Frank, M., Schlüchter, C., 1998. 10Be and 26Al production rates deduced from an instantaneous event within the dendro-calibration curve, the landslide of Köfels, Ötz Valley, Austria. Earth Planet. Sci. Lett. 161, 231–241. https://doi.org/10.1016/S0012-821X(98)00153-8

Kuhlemann, J., 2007. Paleogeographic and paleotopographic evolution of the Swiss and Eastern Alps since the Oligocene. Glob. Planet. Change 58, 224–236. https://doi.org/10.1016/j.gloplacha.2007.03.007

Kuhlemann, J., Frisch, W., Dunkl, I., Székely, B., 2001. Quantifying tectonic versus erosive denudation by the sediment budget: The miocene core complexes of the Alps. Tectonophysics 330, 1–23. https://doi.org/10.1016/S0040-1951(00)00209-2

Kuhlemann, J., Frisch, W., Székely, B., Dunkl, I., Kázmér, M., 2002. Post-collisional sediment budget history of the Alps: Tectonic versus climatic control. Int. J. Earth Sci. 91, 818–837. https://doi.org/10.1007/s00531-002-0266-y

Kühni, A., Pfiffner, O.A., 2001. The relief of the Swiss Alps and adjacent areas and its relation to lithology and structure: Topographic analysis from a 250-m DEM. Geomorphology 41, 285–307. https://doi.org/10.1016/S0169-555X(01)00060-5

Lal, D., Arnold, J.R., 1985. Tracing quartz through the environment. J. Earth Syst. Sci. 94, 1–5. https://doi.org/10.1007/BF02863403

Le Breton, E., Handy, M.R., Molli, G., Ustaszewski, K., 2017. Post-20 Ma Motion of the Adriatic Plate: New Constraints From Surrounding Orogens and Implications for Crust-Mantle Decoupling. Tectonics 36, 3135–3154. https://doi.org/10.1002/2016TC004443

Legrain, N., Stüwe, K., Wölfler, A., 2014a. Incised relict landscapes in the eastern Alps. Geomorphology 221, 124–138. https://doi.org/10.1016/j.geomorph.2014.06.010

Legrain, N., Dixon, J., Stüwe, K., von Blanckenburg, F. V., Kubik, P., 2014b. Post-Miocene landscape rejuvenation at the eastern end of the Alps. Lithosphere 7, 3–13. https://doi.org/10.1130/L391.1

Lippitsch, R., Kissling, E., Ansorge, J., 2003. Upper mantle structure beneath the Alpine orogen from high-resolution teleseismic tomography. J. Geophys. Res. Solid Earth 108, 2376. https://doi.org/10.1029/2002JB002016

Malusà, M.G., Fitzgerald, P.G. (Eds.), 2019. Fission-Track Thermochronology and its Application to Geology, Springer Textbooks in Earth Sciences, Geography and Environment. Springer International Publishing, Cham, (393 pp.). https://doi.org/10.1007/978-3-319-89421-8

Mancktelow, N.S., 1992. Neogene lateral extension during convergence in the Central Alps: Evidence from interrelated faulting and backfolding around the Simplonpass (Switzerland). Tectonophysics 215, 295–317. https://doi.org/10.1016/0040-1951(92)90358-D

Mancktelow, N.S., Stöckli, D.F., Grollimund, B., Müller, W., Fügenschuh, B., Viola, G., Seward, D., Villa, I.M., 2001. The DAV and Pediatriatic fault systems in the Eastern Alps South of the Tauern window. Int. J. Earth Sci. 90, 593–622. https://doi.org/10.1007/s005310000190

Molnar, P., 2004. Late Cenozoic increase in accumulation rates of terrestrial sediment: How might climate change have affected erosion rates? Annu. Rev. Earth Planet. Sci. 32, 67–89. https://doi.org/10.1146/annurev.earth.32.091003.143456

Montgomery, D.R., Korup, O., 2011. Preservation of inner gorges through repeated Alpine glaciations. Nat. Geosci. 4, 62–67. https://doi.org/10.1038/ngeo1030

Mulch, A., 2016. Stable isotope paleoaltimetry and the evolution of landscapes and life. Earth

Planet. Sci. Lett. 433, 180–191. https://doi.org/10.1016/j.epsl.2015.10.034

Nishiizumi, K., Winterer, E.L., Kohl, C.P., Klein, J., Middleton, R., Lal, D., Arnold, J.R., 1989. Cosmic ray production rates of ^{10}Be and ^{26}Al in quartz from glacially polished rocks. J. Geophys. Res. Solid Earth 94, 17907-17915. https://doi.org/10.1029/JB094iB12p17907

Norton, K.P., von Blanckenburg, F., Kubik, P.W., 2010. Cosmogenic nuclide-derived rates of diffusive and episodic erosion in the glacially sculpted upper rhone valley, Swiss Alps. Earth Surf. Process. Landforms 35, 651–662. https://doi.org/10.1002/esp.1961

Norton, K.P., von Blanckenburg, F., Schlunegger, F., Schwab, M., Kubik, P.W., 2008. Cosmogenic nuclide-based investigation of spatial erosion and hillslope channel coupling in the transient foreland of the Swiss Alps. Geomorphology 95, 474–486. https://doi.org/10.1016/j.geomorph.2007.07.013

Perrone, G., Morelli, M., Piana, F., Fioraso, G., Nicolò, G., Mallen, L., Cadoppi, P., Balestro, G., Tallone, S., 2013. Current tectonic activity and differential uplift along the Cottian Alps/Po Plain boundary (NW Italy) as derived by PS-InSAR data. J. Geodyn. 66, 65–78. https://doi.org/10.1016/j.jog.2013.02.004

Qorbani, E., Bianchi, I., Bokelmann, G., 2015. Slab detachment under the Eastern Alps seen by seismic anisotropy. Earth Planet. Sci. Lett. 409, 96–108. https://doi.org/10.1016/j.epsl.2014.10.049

Ratschbacher, L., Frisch, W., Neubauer, F., Schmid, S.M., Neugebauer, J., 1989. Extension in compressional orogenic belts: The eastern Alps. Geology 17, 404–407. https://doi.org/10.1130/0091-7613(1989)017<0404:EICOBT>2.3.CO;2

Ratschbacher, L., Merle, O., Davy, P., Cobbold, P., 1991. Lateral extrusion in the eastern Alps, Part 1: Boundary conditions and experiments scaled for gravity. Tectonics 10, 245–256. https://doi.org/10.1029/90TC02622

Reiners, P.W., Spell, T.L., Nicolescu, S., Zanetti, K.A., 2004. Zircon (U-Th)/He thermochronometry: He diffusion and comparisons with 40Ar/39Ar dating. Geochim. Cosmochim. Acta 68, 1857–1887. https://doi.org/10.1016/j.gca.2003.10.021

Ren, Y., Stuart, G.W., Houseman, G.A., Dando, B., Ionescu, C., Hegedüs, E., Radovanović, S., Shen, Y., 2012. Upper mantle structures beneath the Carpathian-Pannonian region:

Implications for the geodynamics of continental collision. Earth Planet. Sci. Lett. 349–350, 139–152. https://doi.org/10.1016/j.epsl.2012.06.037

Robl, J., Hergarten, S., Stüwe, K., 2008a. Morphological analysis of the drainage system in the Eastern Alps. Tectonophysics 460, 263–277. https://doi.org/10.1016/j.tecto.2008.08.024

Robl, J., Stüwe, K., Hergarten, S., Evans, L., 2008b. Extension during continental convergence in the Eastern Alps: The influence of orogen-scale strike-slip faults. Geology 36, 963–966. https://doi.org/10.1130/G25294A.1

Robl, J., Prasicek, G., Hergarten, S., Stüwe, K., 2015. Alpine topography in the light of tectonic uplift and glaciation. Glob. Planet. Change 127, 34–49. https://doi.org/10.1016/j.gloplacha.2015.01.008

Royden, L., Horváth, F., Rumpler, J., 1983. Evolution of the Pannonian Basin System: 1. Tectonics. Tectonics 2, 63–90. https://doi.org/10.1029/TC002i001p00063

Sadler, P.M., 1999. The Influence of Hiatuses on Sediment Accumulation Rates. GeoResearch Forum 5, 15–40.

Schlatter, A., Schneider, D., Geiger, A., Kahle, H.G., 2005. Recent vertical movements from precise levelling in the vicinity of the city of Basel, Switzerland. Int. J. Earth Sci. 94, 507–514. https://doi.org/10.1007/s00531-004-0449-9

Schlunegger, F., Matter, A., Burbank, D.W., Klaper, E.M., 1997. Magnetostratigraphic constraints on relationships between evolution of the central Swiss Molasse basin and Alpine orogenic events. Bull. Geol. Soc. Am. 109, 225–241. https://doi.org/10.1130/0016-7606(1997)109<0225:MCORBE>2.3.CO;2

Schlunegger, F., Norton, K.P., 2015. Climate vs. tectonics: The competing roles of late oligocene warming and alpine orogenesis in constructing alluvial megafan sequences in the north alpine foreland basin. Basin Res. 27, 230–245. https://doi.org/10.1111/bre.12070

Schmid, S.M., Pfiffner, O.A., Froitzheim, N., Schönborn, G., Kissling, E., 1996. Geophysical-geological transect and tectonic evolution of the Swiss-Italian Alps. Tectonics 15, 1036–1064. https://doi.org/10.1029/96TC00433

Schumer, R., Jerolmack, D.J., 2009. Real and apparent changes in sediment deposition rates

through time. J. Geophys. Res. Solid Earth 114, 1–12. https://doi.org/10.1029/2009JF001266

Schuster, R., Stüwe, K., in print. Geological and Tectonic Setting of Austria, in: Embleton-Hamann, C. (Ed.), Landscapes and Landforms of Austria. Springer, New York, pp. 32.

Şengör, A.M., 2009. The large-wavelength deformations of the lithosphere: Materials for a history of the evolution of thought from the earliest times to plate tectonics, in: The Large-Wavelength Deformations of the Lithosphere: Materials for a History of the Evolution of Thought from the Earliest Times to Plate Tectonics. Geological Society of America Memoirs 196. https://doi.org/10.1130/978-0-8137-1196-7-196.0.1

Serpelloni, E., Vannucci, G., Anderlini, L., Bennett, R.A., 2016. Kinematics, seismotectonics and seismic potential of the eastern sector of the European Alps from GPS and seismic deformation data. Tectonophysics 688, 157–181. https://doi.org/10.1016/j.tecto.2016.09.026

Spiegel, C., Kuhlemann, J., Dunkl, I., Frisch, W., Von Eynatten, H., Balogh, K., 2000. The erosion history of the Central Alps: Evidence from zircon fission track data of the foreland basin sediments. Terra Nov. 12, 163–170. https://doi.org/10.1046/j.1365-3121.2000.00289.x

Sternai, P., Sue, C., Husson, L., Serpelloni, E., Becker, T.W., Willett, S.D., Faccenna, C., Di Giulio, A., Spada, G., Jolivet, L., Valla, P., Petit, C., Nocquet, J.M., Walpersdorf, A., Castelltort, S., 2019. Present-day uplift of the European Alps: Evaluating mechanisms and models of their relative contributions. Earth-Science Rev. 190, 589–604. https://doi.org/10.1016/j.earscirev.2019.01.005

Stille, H., 1919. Die Begriffe Orogenese und Epirogenese. Zeitschrift der Dtsch. Geol. Gesellschaft 71, 164–208.

Stutenbecker, L., Costa, A., Schlunegger, F., 2016. Lithological control on the landscape form of the upper Rhône Basin, Central Swiss Alps. Earth Surf. Dyn. 4, 253–272. https://doi.org/10.5194/esurf-4-253-2016

Stüwe, K., Barr, T.D., 2000. On the relationship between surface uplift and gravitational extension. Tectonics 19, 1056–1064. https://doi.org/10.1029/2000TC900017

Stüwe, K., Homberger, R., 2018. Steiermark aus der Luft. Weishaupt Publishing, Gnas, (208 pp.).

Stüwe, K., Homberger, R., 2012. High above the Alps: A Bird's Eye View of Geology. Weishaupt Publishing, Gnas, (296 pp.).

Sue, C., Delacou, B., Champagnac, J.D., Allanic, C., Tricart, P., Burkhard, M., 2007. Extensional neotectonics around the bend of the Western/Central Alps: An overview. Int. J. Earth Sci. 96, 1101–1129. https://doi.org/10.1007/s00531-007-0181-3

Suess, E., 1883. Das Antlitz der Erde. Bd. Ia (Erste Abtheilung). F. Tempsky, Prag und G. Freytag, Leipzig (310 pp.).

Uehlinger, U., Wantzen, K.M., Leuven, R.S.E.W., Arndt, H., 2009. The Rhine River Basin, in: Tockner, K., Uehlinger, U., Robinson, C.T. (Eds.), Rivers of Europe. Elsevier Ltd, pp. 199–245. https://doi.org/10.1016/B978-0-12-369449-2.00006-0

Valla, P.G., Shuster, D.L., Van Der Beek, P.A., 2011. Significant increase in relief of the European Alps during mid-Pleistocene glaciations. Nat. Geosci. 4, 688–692. https://doi.org/10.1038/ngeo1242

Vernon, A.J., van der Beek, P.A., Sinclair, H.D., Rahn, M.K., 2008. Increase in late Neogene denudation of the European Alps confirmed by analysis of a fission-track thermochronology database. Earth Planet. Sci. Lett. 270, 316–329. https://doi.org/10.1016/j.epsl.2008.03.053

von Blanckenburg, F., 2005. The control mechanisms of erosion and weathering at basin scale from cosmogenic nuclides in river sediment. Earth Planet. Sci. Lett. 237, 462–479. https://doi.org/10.1016/j.epsl.2005.06.030

von Blanckenburg, F., Davies, J.H., 1995. Slab breakoff: A model for syncollisional magmatism and tectonics in the Alps. Tectonics 14, 120–131. https://doi.org/10.1029/94TC02051

Wagner, T., Fabel, D., Fiebig, M., Häuselmann, P., Sahy, D., Xu, S., Stüwe, K., 2010. Young uplift in the non-glaciated parts of the Eastern Alps. Earth Planet. Sci. Lett. 295, 159–169. https://doi.org/10.1016/j.epsl.2010.03.034

Wagner, T., Fritz, H., Stüwe, K., Nestroy, O., Rodnight, H., Hellstrom, J., Benischke, R., 2011. Correlations of cave levels, stream terraces and planation surfaces along the River Mur-Timing of landscape evolution along the eastern margin of the Alps. Geomorphology 134, 62–78. https://doi.org/10.1016/j.geomorph.2011.04.024

Walpersdorf, A., Sue, C., Baize, S., Cotte, N., Bascou, P., Beauval, C., Collard, P., Daniel, G., Dyer, H., Grasso, J.R., Hautecoeur, O., Helmstetter, A., Hok, S., Langlais, M., Menard, G., Mousavi, Z., Ponton, F., Rizza, M., Rolland, L., Souami, D., Thirard, L., Vaudey, P., Voisin, C., Martinod, J., 2015. Coherence between geodetic and seismic deformation in a context of slow tectonic activity (SW Alps, France). J. Geodyn. 85, 58–65. https://doi.org/10.1016/j.jog.2015.02.001

Weber, J., Vrabec, M., Pavlovčič-Prešeren, P., Dixon, T., Jiang, Y., Stopar, B., 2010. GPS-derived motion of the Adriatic microplate from Istria Peninsula and Po Plain sites, and geodynamic implications. Tectonophysics 483, 214–222. https://doi.org/10.1016/j.tecto.2009.09.001

Wegener, A., 1912. Die Entstehung der Kontinente. Geol. Rundschau 3, 276–292, and Petermanns Geogr. Mitteil. 58(1), 185–195, 253–256, 305–309

Willenbring, J.K., von Blanckenburg, F., 2010. Long-term stability of global erosion rates and weathering during late-Cenozoic cooling. Nature 465, 211–214. https://doi.org/10.1038/nature09044

Willett, S.D., 2010. Late Neogene Erosion of the Alps: A Climate Driver? Annu. Rev. Earth Planet. Sci. 38, 411–437. https://doi.org/10.1146/annurev-earth-040809-152543

Willett, S.D., Schlunegger, F., Picotti, V., 2006. Messinian climate change and erosional destruction of the central European Alps. Geology 34, 613–616. https://doi.org/10.1130/G22280.1

Winkler-Hermaden, A., 1957. Geologisches Kräftespiel und Landformung. Springer Verlag, Vienna.

Wittmann, H., Malusà, M.G., Resentini, A., Garzanti, E., Niedermann, S., 2016. The cosmogenic record of mountain erosion transmitted across a foreland basin: Source-to-sink analysis of in situ 10Be, 26Al and 21Ne in sediment of the Po river catchment. Earth

Planet. Sci. Lett. 452, 258–271. https://doi.org/10.1016/j.epsl.2016.07.017

Wittmann, H., von Blanckenburg, F., Kruesmann, T., Norton, K.P., Kubik, P.W., 2007. Relation between rock uplift and denudation from cosmogenic nuclides in river sediment in the Central Alps of Switzerland. J. Geophys. Res. Earth Surf. 112, 1–20. https://doi.org/10.1029/2006JF000729

Wobus, C., Whipple, K.X., Kirby, E., Snyder, N., Johnson, J., Spyropolou, K., Crosby, B., Sheehan, D., 2006. Tectonics from topography: Procedures, promise, and pitfalls, in: Willet, S.D., Hovius, N., Brandon, M.T., Fisher, D.M. (Eds), Tectonics, Climate, and Landscape Evolution. Geol. Soc. Am. Special Paper 398, pp. 55-74. https://doi.org/10.1130/2006.2398(04)

Wölfler, A., Kurz, W., Fritz, H., Stüwe, K., 2011. Lateral extrusion in the Eastern Alps revisited: Refining the model by thermochronological, sedimentary, and seismic data. Tectonics 30, TC4006. https://doi.org/10.1029/2010TC002782

Wölfler, A., Stüwe, K., Danišík, M., Evans, N.J., 2012. Low temperature thermochronology in the Eastern Alps: Implications for structural and topographic evolution. Tectonophysics 541–543, 1–18. https://doi.org/10.1016/j.tecto.2012.03.016

Zachos, J., Pagani, H., Sloan, L., Thomas, E., Billups, K., 2001. Trends, rhythms, and aberrations in global climate 65 Ma to present. Science 292, 686–693. https://doi.org/10.1126/science.1059412

Appendix: Channel Profile Analysis of Major Alpine Drainages

Analyzing landscape morphology for the purpose of inferring aspects of the geological uplift and erosion history using channel profiles and slope elevation criteria as used in Fig. 3 of this thesis, is a modern quantitative tool used by many tectonic geomorphologists (e.g. Kirby and Whipple, 2001; Cyr et al., 2014; Bartosch and Stüwe, 2019). In this appendix, I will illustrate the method and present some new results for the major drainages of the Alps.

Method

The principle of analyzing longitudinal river profiles is based on Flint's Law following a stream-power approach:

$$S = \left(\frac{u}{k}\right)^{\frac{1}{n}} A^{\frac{-m}{n}} = k_s A^{-\theta}, \quad (1)$$

where S is the slope, A is the upstream catchment area, k_s is called the steepness index, θ is called the concavity index, u is the uplift rate, k is the erodibility, m and n are positive constants representing basin hydrology, hydraulic geometry and incision process and are also called area exponent and slope exponent, respectively (Flint, 1974; Whipple and Tucker, 1999; Wobus et al., 2006; Hergarten et al., 2016). Since k_s autocorrelates with θ, the normalized steepness index k_{sn} is calculated using a reference concavity of $\theta_{ref} = 0.45$ in order to compare streams with different concavities (Wobus et al., 2006).

If a stream is in equilibrium (uniform u, k, m and n), a double logarithmic plot of S against A displays a linear regression trend. When glacial imprint as well as variations in precipitation and sediment load are negligible, then deviations of this linear regression trend can be interpreted in terms of uplift and erodibility. Such deviations are termed knickpoints. To deduce the origin of these knickpoints, they have to be defined as either static or dynamic knickpoints. A static knickpoint has a fixed position along the stream and usually correlates with lithological boundaries, i.e. a change in erodibility k. A dynamic knickpoint on the other hand is not bound to one location but will migrate upstream and is typically caused by variations in uplift rate u. Either of these scenarios should be depicted by a change in k_{sn} along the channel profile. However, changes in u and k can lead to very similar trends. Therefore, it can be useful to compare changes in k_{sn} with in-situ measured erosion rates (Cyr et al., 2014). To reduce topographic noise, a chi-transformation after Perron and Royden (2013) can be performed, using a normalized area and concavity. With this changed horizontal component, a stream in

equilibrium results in a linear elevation-chi trend and the curves steepness may be interpreted in terms of uplift rate (Perron and Royden, 2013).

Orogen-scale application of channel profiles

In order to derive aspects of the uplift history of the Alps, the logic explained above was applied to some of the largest drainages in the Alpine realm. Channel profiles of four major rivers of the Alps, namely the Po, Rhône, Rhine and Danube, were created with TopoToolbox (Schwanghart and Kuhn, 2010) using a 30 m DEM. Fig. A1 shows recent uplift rates interpreted from Sternai et al. (2019) with all important locations that are discussed in this chapter and the drainage network of the discussed rivers.

The Po has its source in the Dora-Maira Massif on the Italian side of the Western Alps and crosses the Po Plain from west to east until it finally enters the Adriatic Sea 50 km south of Venice. Its longitudinal channel profile shows three distinct knickpoints which show in differences in k_{sn}, changes in slope-area regression and elevation-chi plot. The first one shows a sudden decrease in channel slope, which aligns well with the transition from the metamorphic rocks of the Dora-Maira Massif to the Quaternary sediments of the Po Plain. The very low k_{sn} values at the beginning of the Po Plain indicate either decreased uplift rate or higher erodibility. A lower uplift rate, as also indicated by the decreasing slope of the elevation-chi curve, is also supported by the observed uplift rates for this area, showing subsidence for the westernmost Po Plain (Fig. A1; Perrone et al., 2013). However, the obvious change in lithology and therefore change in erodibility suggests a static knickpoint due to lithological control, although the influence of the recent subsidence can not be negated. The second knickpoint is located near Torino and is marked by a sudden increase in channel slope. Increased uplift rates downstream indicated by higher k_{sn} values and a steeper elevation-chi curve are supported by GPS and InSAR measurements (Fig. A1; Perrone et al., 2013). The knickpoint location aligns with the intersection of Po and the Padanian Thrust Front, which exhumed the Cenozoic rocks east of Torino, and will eventually migrate headwards (Cyr et al., 2014). The lithology is uniform with the last channel section, ruling out lithological control over this knickpoint. The third knickpoint around the city of Piacenza can barely be seen at this resolution, yet it shows a similar step-shape in the channel profile to the second one. While little more information can be extracted from Fig. A2, Fig. A1 displays an area of accelerated uplift right downstream of Piacenza. The region of the Apennine front is tectonically active and most probably the reason for the increased vertical motion in this area (Boccaletti et al., 2011).

The source of the Rhône lies at the toe of the Rhône glacier in the Swiss Alps, which immediately brings to attention that an interpretation of its channel profile might not be viable since the Rhône valley was heavily glaciated during the Pleistocene glaciation cycles (e.g. Ivy-Ochs et al., 2008). The strong scatter in the slope-area plot is most probably due to the glacial impact and any fitted regressions should be handled with doubt (Fig. A3). After the first 6.5 km, the Rhône has already experienced an elevation loss of over 800 m and shows a concave step in the channel profile. This step marks the entry from the former tributary glacier into the actual Rhône valley. At the knickpoint at the town of Visp, the Rhône runs no more on the Mesozoic sedimentary cover of the allochthone massifs, but on Quaternary sediments, marking a distinct change in erodibility. It is also the location where the Rhône-Simplon Fault merges into the Rhône valley. The next knickpoint coincides roughly with a change to slightly less erodible lithology (Kühni and Pfiffner, 2001). The knickpoint a few kilometres before Lake Geneva does not show any discrepancy in erodibility and further interpretations will be left aside. Downstream of Lake Geneva, many hydroelectric powerplants with dams up to 100 m in height disrupt the natural flow of the Rhône. The LGM extent terminates around the city of Lyon. The scatter of slopes reduces downstream of Lyon and the elevation-chi plot shows a much more linear trend. This nicely shows the disrupting influence of glaciation on stream profiles. However, slopes are increasing again with a knickpoint ~ 90 km downstream of Lyon, which may be attributed to the drop in base level during the Messinian (Gargani, 2004).

The Rhine, although having its source only 20 km east of the Rhône glacier, shows a completely different channel profile (Fig. A4). Compared to the Po and the Rhône the Rhine appears to be somewhat equilibrated, even though the Rhine valley was glaciated during the LGM. There are no major jumps in slope and the elevation-chi curve has two almost linear sections with slightly different trends, interrupted by Lake Constance. These two sections equilibrate to two different base levels, being Lake Constance for the upstream section and the Rhine Graben for the downstream section of Lake Constance (Uehlinger et al., 2009).

The Danube is the only major drainage of the Alps that does not actually originate in the Alps. The longitudinal channel profile starts at the official source of the Danube in Donaueschingen (Fig. A5). Similar to the lower Rhône valley, the Danube inherits a vast number of hydroelectric powerplants that are represented by the many flat steps in the channel profile. The best fit for a slope-area regression appears rather poorly. However, when looking at the elevation-chi plot, two sections with linear trends and different slopes are visible. This also shows in the k_{sn} values. The change from lower k_{sn} upstream to higher k_{sn} downstream correlates well with the boundary from the Molasse Basin to the crystalline rocks of the Bohemian Massif. This marks

a distinct change in erodibility. However, the k_{sn} values remain relatively high when the Danube re-enters the Molasse Basin at the city of Krems and only drop again already 100 km in the Vienna Basin. This might indicate an increased uplift rate compared to the western part of the Molasse Basin. The fact that the Danube is an antecedent river which cuts through the comparably erosion-resistant Bohemian Massif instead of following the path of least resistance through the Molasse Basin also supports the idea of a young uplift event of the region.

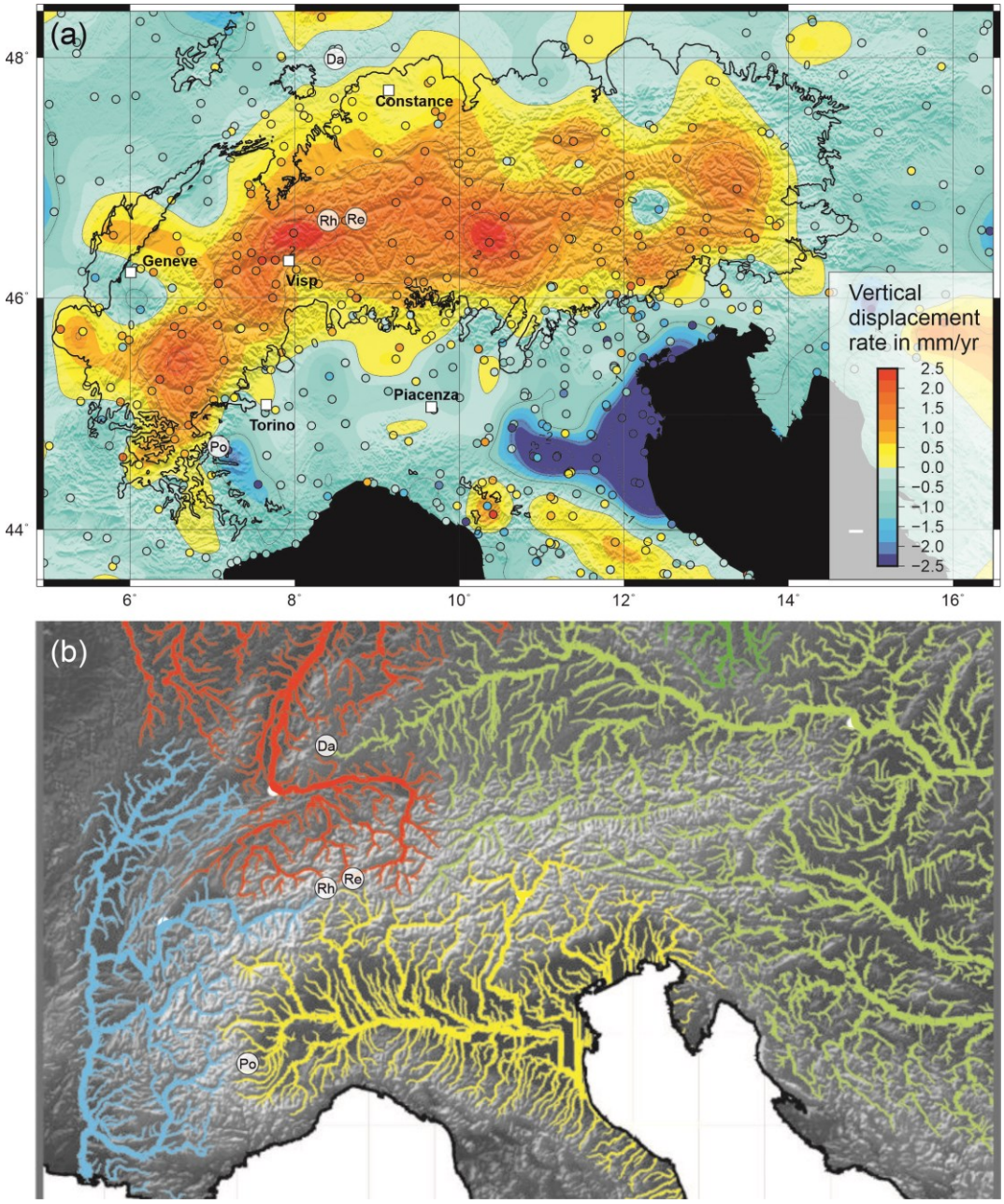

Fig. A1: Two maps providing a geographic framework of Po, Rhône, Rhine and Danube. (a) Present-day vertical displacement rates measured with GPS/GNSS across the Alps, modified from the interpretation of Sternai et al. (2019). Circles indicate the location of the measuring GPS/GNSS stations. White rectangles mark important locations discussed in the text. Transparent circles indicate the sources of the discussed drainages (Po = Po; Rh = Rhône; Re = Rhine; Da = Danube). (b) Drainage network of Po (yellow), Rhône (blue), Rhine (red) and Danube (green).

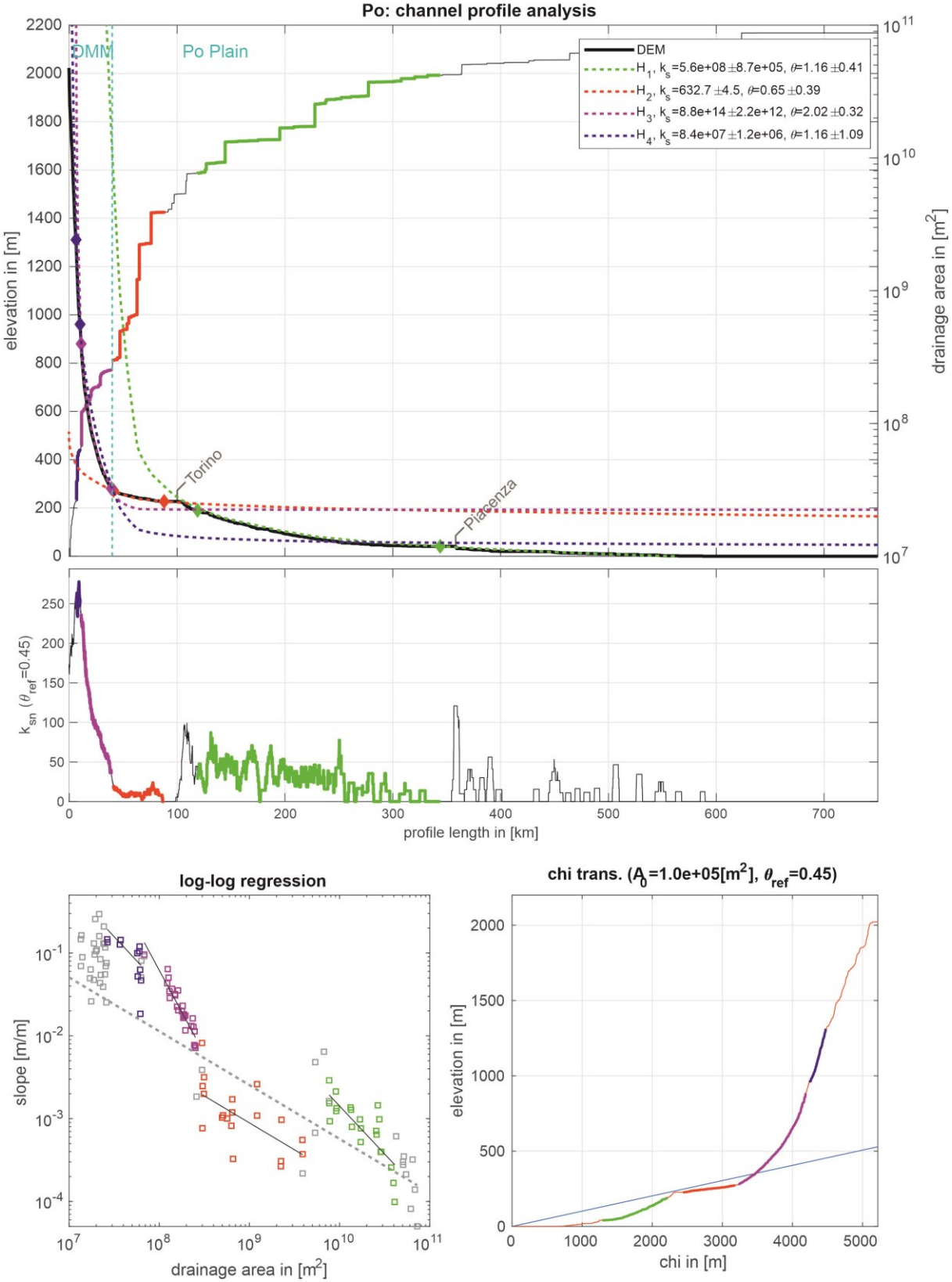

Fig. A2: Longitudinal channel profile of the Po river, including k_{sn} values over profile length, double logarithmic plot of slope and drainage area and chi-elevation plot. Along the profile, the locations of cities and lithological changes (DMM = Dora-Maira Massif) important for the interpretation are indicated. The different colors (green, red, magenta, blue) each represent projected equilibrium segments of the stream. For further information see text.

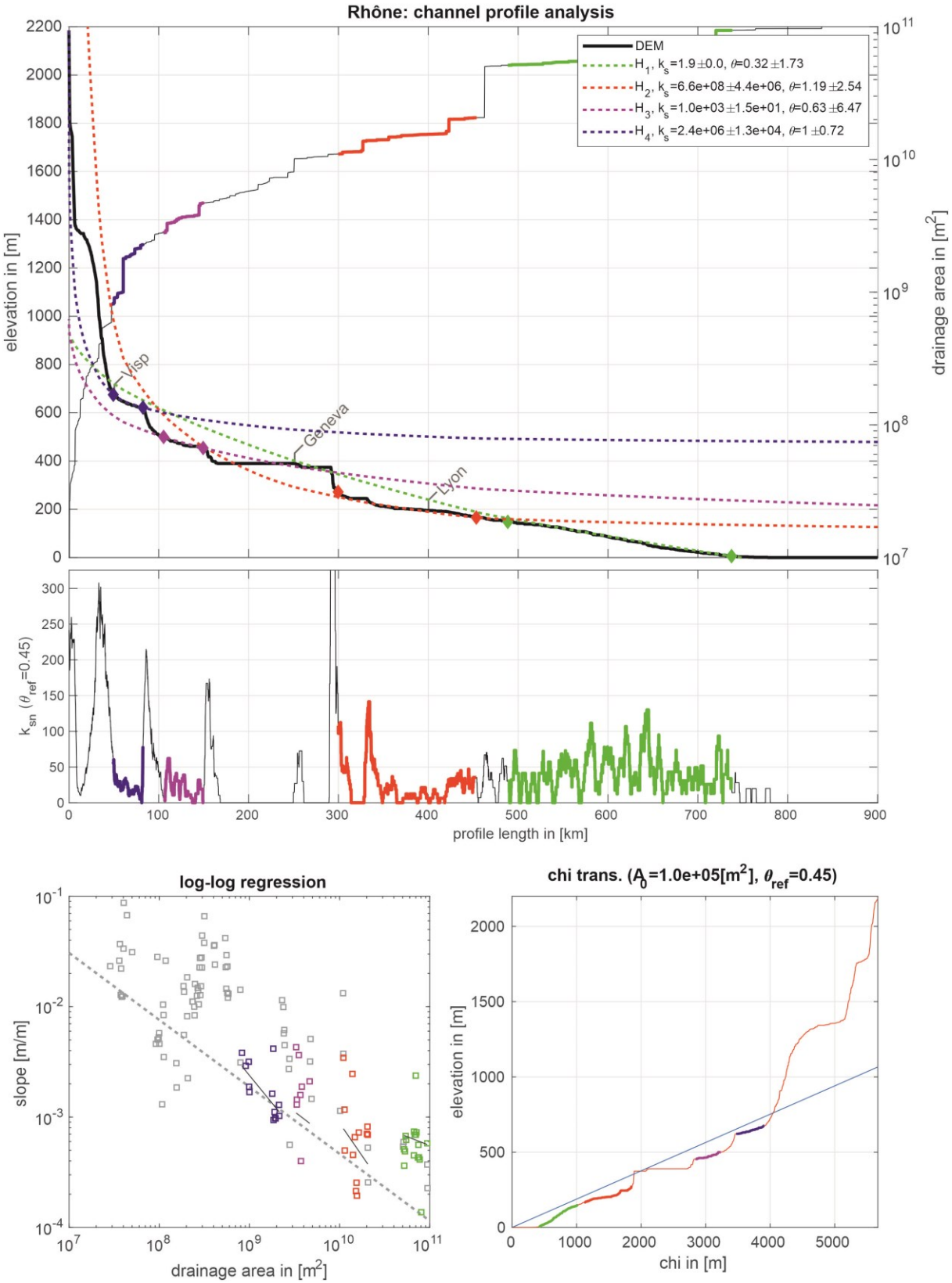

Fig. A3: Longitudinal channel profile of the Rhône river, including k_{sn} values over profile length, double logarithmic plot of slope and drainage area and chi-elevation plot. Along the profile, the locations of towns and cities important for the interpretation are indicated. The different colors (green, red, magenta, blue) each represent projected equilibrium segments of the stream. For further information see text.

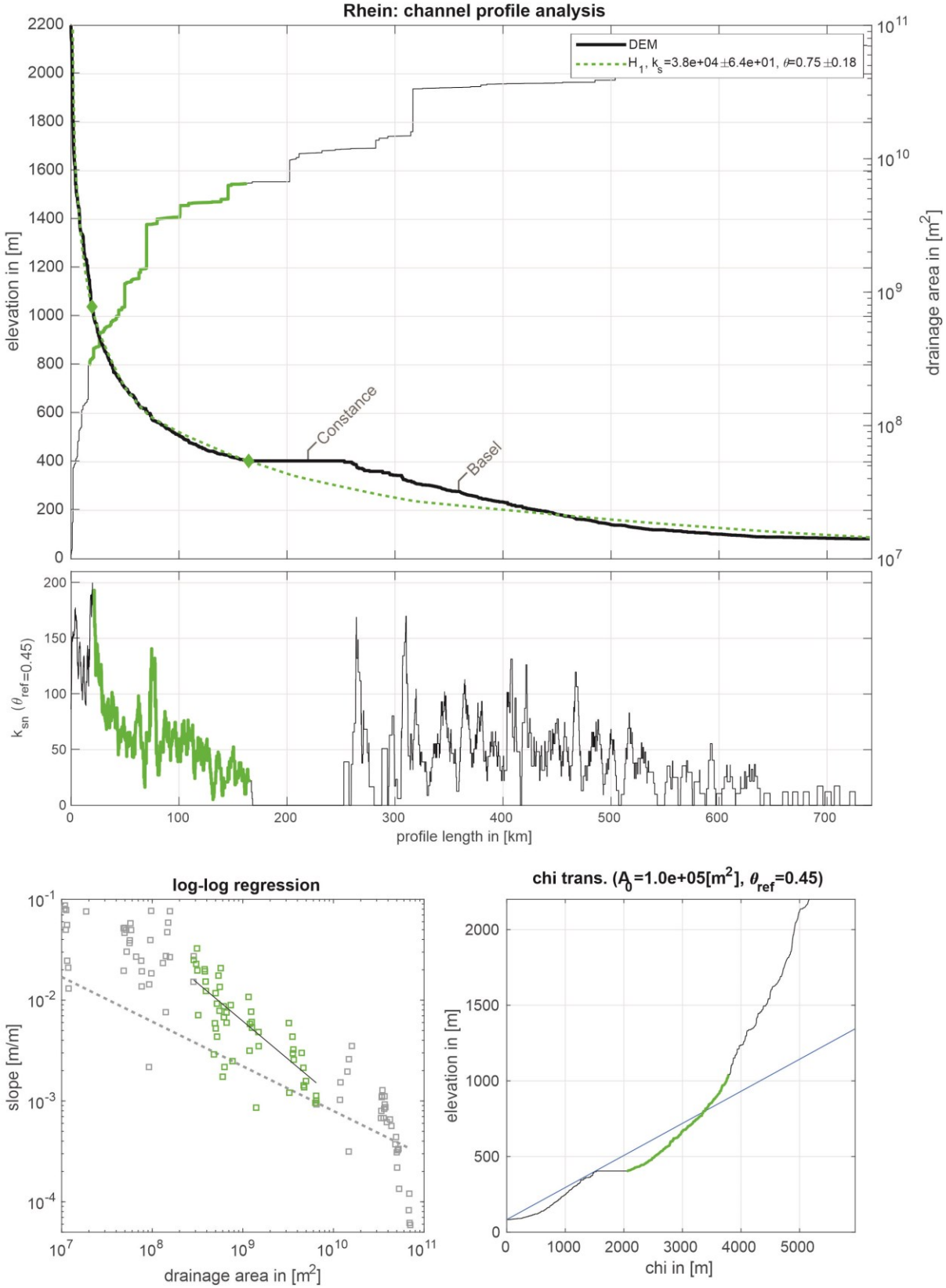

Fig. A4: Longitudinal channel profile of the Rhine river, including k_{sn} values over profile length, double logarithmic plot of slope and drainage area and chi-elevation plot. Along the profile, the locations of towns and cities important for the interpretation are indicated. Only one equilibrium curve (green) could be generated. For further information see text.

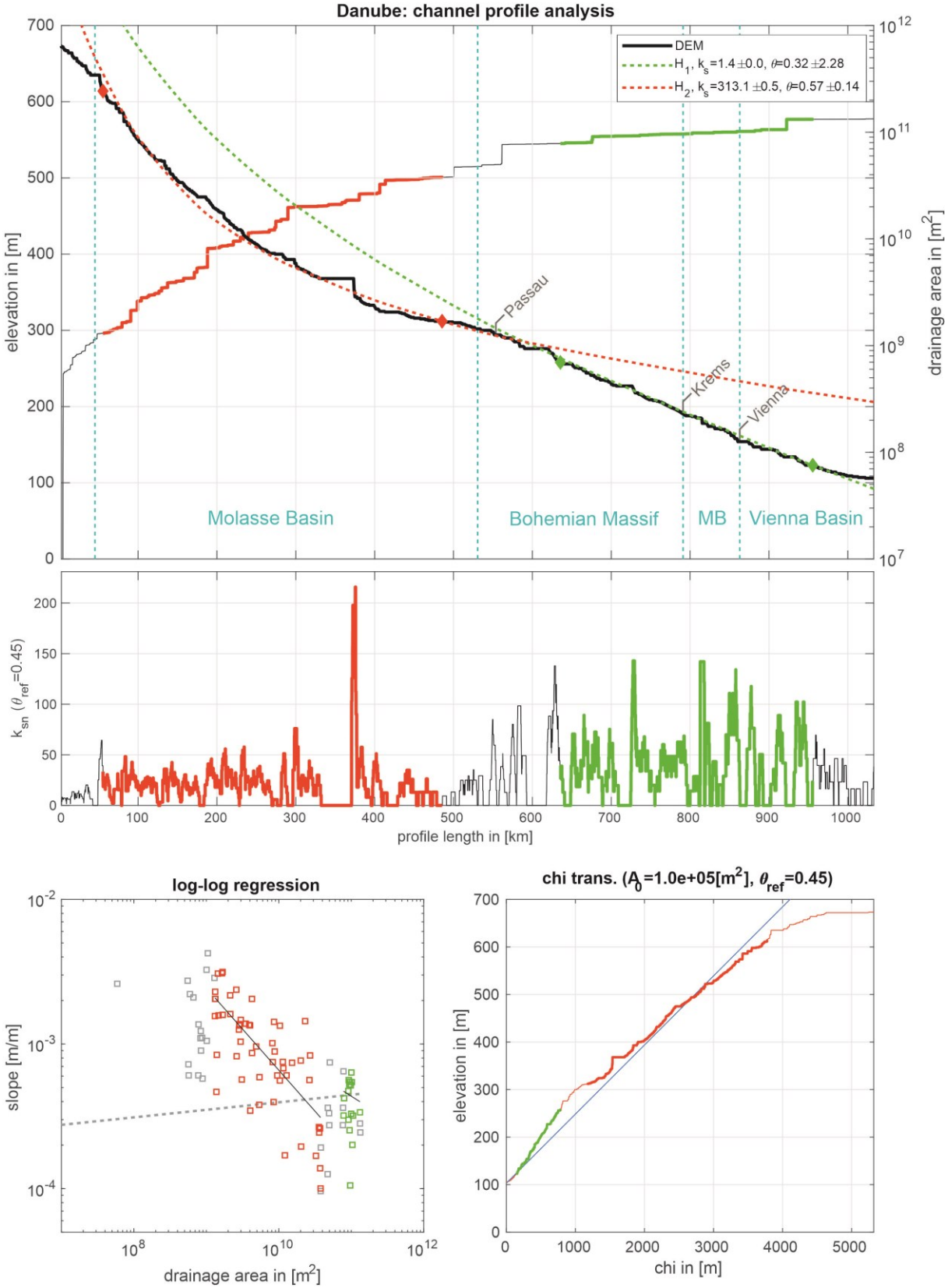

Fig. A5: Longitudinal channel profile of the Danube river, including k_{sn} values over profile length, double logarithmic plot of slope and drainage area and chi-elevation plot. Along the profile, the locations of cities and lithological changes (MB = Molasse Basin) important for the interpretation are indicated. The different colors (green, red) each represent projected equilibrium segments of the stream. For further information see text.

Conclusions

The analyzation of longitudinal river profiles an orogen-wide scale is a useful tool to gather information about the evolution of topography and landscapes. By looking at the channel profiles of the four major drainages of the Alps, I came to the following conclusions.

- Along the Po, two zones of accelerated young uplift can be found. Both, the region downstream of Torino and the region downstream of Piacenza, have been subject to post-Miocene transpressive tectonics (Perrone et al., 2013; Boccaletti et al., 2011).
- The Bohemian Massif and the eastern Molasse Basin experienced a young uplift pulse, which is not resolved in the western Molasse Basin. Apart from headwater-catchments getting subsequently captured by the Rhine (Robl et al., 2008), the course of the Danube did not experience a major reorganization since the end of the Miocene.
- The Rhine appears to be in geomorphic equilibrium until Lake Constance. The different base levels of Lake Constance and the Rhine Graben is not a result of uplift but rather of subsidence of the Rhine Graben.
- Although glacially overprinted, the knickpoints along the upper Rhône channel profile can mostly be attributed to lithologic differences, as already submitted by Stutenbecker et al. (2016). However, some features can not be explained by lithologic factors alone, but the strong scatter of the data points does not allow further meaningful interpretations.
- The knickpoint of the lower Rhône ~ 90 km downstream of Lyon is caused by the equilibration of the sections above and below it to different base levels. This is most probably due to base level fluctuations since the Messinian (Gargani, 2004).
- The alteration of rivers by human interferences must not be underestimated when interpreting channel profiles, as prominently visible in the Rhône, where the second most conspicuous feature after Lake Geneva is the Génissiat Dam 40 km downstream of the lake.

References

Bartosch, T., Stüwe, K., 2019. Evidence for pre-pleistocene landforms in the eastern alps: Geomorphological constraints from the gurktal alps. Austrian J. Earth Sci. 112, 84–102. https://doi.org/10.17738/ajes.2019.0006

Boccaletti, M., Corti, G., Martelli, L., 2011. Recent and active tectonics of the external zone of the Northern Apennines (Italy). Int. J. Earth Sci. 100, 1331–1348. https://doi.org/10.1007/s00531-010-0545-y

Cyr, A.J., Granger, D.E., Olivetti, V., Molin, P., 2014. Distinguishing between tectonic and lithologic controls on bedrock channel longitudinal profiles using cosmogenic 10Be erosion rates and channel steepness index. Geomorphology 209, 27–38. https://doi.org/10.1016/j.geomorph.2013.12.010

Flint, J.J., 1974. Stream gradient as a function of order, magnitude, and discharge. Water Resour. Res. 10, 969–973. https://doi.org/10.1029/WR010i005p00969

Gargani, J., 2004. Modelling of the erosion in the Rhone valley during the Messinian crisis (France). Quat. Int. 121, 13–22. https://doi.org/10.1016/j.quaint.2004.01.020

Hergarten, S., Robl, J., Stuwe, K., 2016. Tectonic geomorphology at small catchment sizes - extensions of the stream-power approach and the x method. Earth Surf. Dyn. 4, 1–9. https://doi.org/10.5194/esurf-4-1-2016

Ivy-Ochs, S., Kerschner, H., Reuther, A., Preusser, F., Heine, K., Maisch, M., Kubik, P.W., Schlüchter, C., 2008. Chronology of the last glacial cycle in the European Alps. J. Quat. Sci. 23, 559–573. https://doi.org/10.1002/jqs.1202

Kirby, E., Whipple, K., 2001. Quantifying differential rock-uplift rates via stream profile analysis. Geology 29, 415–418. https://doi.org/10.1130/0091-7613(2001)029<0415:QDRURV>2.0.CO;2

Kühni, A., Pfiffner, O.A., 2001. The relief of the Swiss Alps and adjacent areas and its relation to lithology and structure: Topographic analysis from a 250-m DEM. Geomorphology 41, 285–307. https://doi.org/10.1016/S0169-555X(01)00060-5

Perron, J.T., Royden, L., 2013. An integral approach to bedrock river profile analysis. Earth Surf. Process. Landforms 38, 570–576. https://doi.org/10.1002/esp.3302

Perrone, G., Morelli, M., Piana, F., Fioraso, G., Nicolò, G., Mallen, L., Cadoppi, P., Balestro, G., Tallone, S., 2013. Current tectonic activity and differential uplift along the Cottian Alps/Po Plain boundary (NW Italy) as derived by PS-InSAR data. J. Geodyn. 66, 65–78. https://doi.org/10.1016/j.jog.2013.02.004

Robl, J., Hergarten, S., Stüwe, K., 2008. Morphological analysis of the drainage system in the

Eastern Alps. Tectonophysics 460, 263–277. https://doi.org/10.1016/j.tecto.2008.08.024

Schwanghart, W., Kuhn, N.J., 2010. TopoToolbox: A set of Matlab functions for topographic analysis. Environ. Model. Softw. 25, 770–781. https://doi.org/10.1016/j.envsoft.2009.12.002

Stutenbecker, L., Costa, A., Schlunegger, F., 2016. Lithological control on the landscape form of the upper Rhône Basin, Central Swiss Alps. Earth Surf. Dyn. 4, 253–272. https://doi.org/10.5194/esurf-4-253-2016

Uehlinger, U., Wantzen, K.M., Leuven, R.S.E.W., Arndt, H., 2009. The Rhine River Basin, in: Tockner, K., Uehlinger, U., Robinson, C.T. (Eds.), Rivers of Europe. Elsevier Ltd, pp. 199–245. https://doi.org/10.1016/B978-0-12-369449-2.00006-0

Whipple, K.X., Tucker, G.E., 1999. Dynamics of the stream-power river incision model: Implications for height limits of mountain ranges, landscape response timescales, and research needs. J. Geophys. Res. Solid Earth 104, 17661–17674. https://doi.org/10.1029/1999JB900120

Wobus, C., Whipple, K.X., Kirby, E., Snyder, N., Johnson, J., Spyropolou, K., Crosby, B., Sheehan, D., 2006. Tectonics from topography: Procedures, promise, and pitfalls, in: Willet, S.D., Hovius, N., Brandon, M.T., Fisher, D.M. (Eds), Tectonics, Climate, and Landscape Evolution. Geol. Soc. Am. Special Paper 398, pp. 55-74. https://doi.org/10.1130/2006.2398(04)